

Discretizations of surfaces with constant ratio of principal curvatures

Michael R. Jimenez · Christian Müller · Helmut Pottmann

the date of receipt and acceptance should be inserted later

Abstract Motivated by applications in architecture, we study surfaces with a constant ratio of principal curvatures. These surfaces are a natural generalization of minimal surfaces and can be constructed by a Christoffel-type transformation from appropriate spherical curvature line parametrizations, both in the smooth setting and in a discretization with principal nets. We link this Christoffel-type transformation to the discrete curvature theory for parallel meshes and characterize nets that allow for these transformations. In the case of negative curvature, we also present a discretization based on asymptotic nets. It is suitable for design and computation and forms the basis for a special type of architectural support structures which can be built by bending flat rectangular strips of inextensible material such as sheet metal.

1 Introduction

The motivation for this research comes from architectural geometry [16], an area that deals with geometric and computational problems related to the realization of geometric complexity in architecture. In particular, the realization of architectural freeform structures is a big challenge. One problem in this context is the design of support structures that are formed by curved beams along freeform surfaces realizing façades and roofs. Our work is motivated by a remarkable instance of such structures, developed by Eike Schling and Denis Hitrec at TU Munich (see Fig. 1). These structures are formed by developable strips, which are orthogonal to a minimal surface S and aligned with a grid of asymptotic curves of S . This implies that the asymptotic curves of S are geodesics on the developable strips and thus the structure can be built from rectangular planar strips of sheet metal. Asymptotic directions on a minimal surface are orthogonal and thus the structures exhibit right node angles at the intersections of strips (which are usually within tolerance to straight line segments).

We are interested in a generalization of these structures. They shall be formed by developable strips with a rectangular development, orthogonal to a base surface S , and the node angles should be constant, but not necessarily right ones. Hence, the base surface S must have a constant angle between asymptotic directions, and therefore negative Gaussian curvature $K < 0$ and a constant ratio κ_1/κ_2 of principal curvatures.

Another problem in architectural geometry is the coverage of a freeform surface with panels [6]. It is an advantage if multiple curved panels can be built with the same mold. A surface with constant κ_1/κ_2 has

All authors
TU Wien, Institute for Discrete Mathematics and Geometry
Wiedner Hauptstraße 8-10/104, A-1040 Vienna
E-mail: michael.jimenez@tuwien.ac.at, christian.mueller@tuwien.ac.at, helmut.pottmann@tuwien.ac.at



Fig. 1 The INSIDE-OUT pavilion by Schling and Hitrec on the campus of TU Munich (image: Felix Noe)

just a one-parameter family of second order surface elements and thus there is the hope that one can find a panelization which uses only a rather small number of molds. Here, also the case $K > 0$ is of interest.

1.1 Previous work.

Despite the simple definition, there is surprisingly little knowledge on surfaces with constant κ_1/κ_2 , except for $\kappa_1/\kappa_2 = \pm 1$, i.e., the sphere and minimal surfaces.

Another known case is an ideal *Mylar ballon* (see e.g., [13, 14]) which is obtained by gluing two equally sized discs of flexible but inextensible foil along their common border and blowing it up. This particular surface of revolution has a constant ratio of principal curvatures of $\kappa_1/\kappa_2 = 2$. Further surfaces of revolution of that sort with positive and negative ratios of principal curvatures have appeared in other contexts, e.g., in [9, 11].

In architectural geometry, basic differential geometric and computational aspects of curved support structures from developable strips have been studied by Tang et al. [20].

1.2 Contributions and overview

Since there is little known on smooth surfaces with a constant ratio of principal curvatures, we first study those in Section 2. The focus is on a novel Christoffel-type transformation which generates these surfaces from appropriate spherical curvature-line parametrizations.

In Section 3 we present a discretization of the smooth Christoffel-type transformation in the setting of discrete conjugate nets and characterize those which allow for these type of transformations. We apply these transformations to spherical principal nets to obtain discretized nets with a constant ratio of principal curvatures in an appropriate sense. We also show that our discrete nets fulfill the characterizing equation for surfaces with constant ratio of principal curvatures in terms of a particular discrete curvature theory.

In Section 4 we turn to a discretization based on asymptotic nets which fits well to a recently proposed optimization framework for exploring the solution space of underdetermined systems of at-most quadratic constraints [22]. We also show how to handle the available degrees of freedom, or in other words, to generate appropriate input for design. Finally, we provide a few illustrative examples for support structures with a constant node angle.

2 Smooth surfaces

Before we start to investigate discretizations of surfaces with a constant ratio of principal curvatures, we analyze properties of the corresponding smooth surfaces, some of which we will discretize later.

To make our formulas look more symmetric we introduce two real values $\alpha, \beta \in \mathbb{R} \setminus \{0\}$ such that our characterizing equation becomes

$$\frac{\kappa_1}{\kappa_2} = \frac{\beta}{\alpha} \quad \text{or} \quad \alpha \kappa_1 = \beta \kappa_2. \quad (1)$$

2.1 Weingarten surfaces

A surface whose curvature radii $r_1 = \kappa_1^{-1}, r_2 = \kappa_2^{-1}$ are related by an equation of the form

$$W(r_1, r_2) = 0$$

are so called *Weingarten surfaces*. From Equation (1) follows immediately that surfaces with a constant ratio of principal curvatures are Weingarten surfaces since here the characterizing equation is the linear equation $W(r_1, r_2) = \beta r_1 - \alpha r_2 = 0$. Any equation for the curvature radii which characterizes Weingarten surfaces can be rewritten in terms of the Gaussian curvature $K = \kappa_1 \kappa_2$ and mean curvature $H = \frac{1}{2}(\kappa_1 + \kappa_2)$ since the principal curvatures can be expressed in terms of Gaussian and mean curvature as $\kappa_1 = H + \sqrt{H^2 - K}$ and $\kappa_2 = H - \sqrt{H^2 - K}$. Consequently, Equation (1) can be rewritten as

$$\alpha(H + \sqrt{H^2 - K}) = \beta(H - \sqrt{H^2 - K}),$$

and after rearranging and squaring, Equation (1) becomes

$$4\alpha\beta H^2 - (\alpha + \beta)^2 K = 0, \quad \text{or} \quad \frac{H^2}{K} = \frac{(\alpha + \beta)^2}{4\alpha\beta} = \text{const.} \quad (2)$$

2.2 A Christoffel-type transformation

In this section, we would like to study a particular type of transformation of conjugate nets $f : \mathbb{R}^2 \rightarrow \mathbb{R}^3$ autonomously from the theory of surfaces with a constant ratio of principal curvatures. In Section 2.3 we will bridge to our main topic and make a connection to the famous Christoffel transformation [5].

First, let us shortly remind what conjugacy means. Two tangent vectors a, b in the tangent plane $T_p f$ are said to be *conjugate*, if they are orthogonal with respect to the second fundamental form. Consequently, if a and b are expressed as a linear combination of the principal directions then conjugacy means $a^\top \begin{pmatrix} \kappa_1 & 0 \\ 0 & \kappa_2 \end{pmatrix} b = 0$. The map which maps a tangent through p in the tangent plane $T_p f$ to its conjugate tangent is an involutive projective automorphism of the line pencil through p , the *involution of conjugate lines*.

A *conjugate net* is then a parametrization of a surface where in each point the tangents to the parameter lines are conjugate.

Let us consider two conjugate nets $f, f^* : \mathbb{R}^2 \rightarrow \mathbb{R}^3$ and $\alpha, \beta \in \mathbb{R} \setminus \{0\}$. The two conjugate nets are said to be *parallel* or *related by a Combescure transformation* if at each point the partial derivatives are parallel, i.e., $f_u \parallel f_u^*$ and $f_v \parallel f_v^*$.

Thus a particular case of Combescure transformations is governed by

$$f_u^* = \frac{\alpha}{\lambda^2} f_u \quad \text{and} \quad f_v^* = \frac{\beta}{\lambda^2} f_v, \quad (3)$$

for some $\lambda : \mathbb{R}^2 \rightarrow \mathbb{R}_{>0}$. The existence of f^* and λ for a given conjugate net f such that the system of PDE's (3) is integrable is equivalent to the existence of λ fulfilling the integrability condition $f_{uv}^* = f_{vu}^*$ and therefore

$$(\alpha - \beta)f_{uv} = 2\alpha(\log \lambda)_v f_u - 2\beta(\log \lambda)_u f_v. \quad (4)$$

Note that the assumption of f being a conjugate net would actually also be a consequence of Equation (4) without requiring it.

Consequently, assuming f additionally to be an orthogonal net, i.e., $f_u \perp f_v$ everywhere, implies that f is a curvature-line parametrization. Note that orthogonality would follow again automatically if we would assume f to be spherical, because all conjugate nets on the sphere are orthogonal. Therefore, also assuming orthogonality we obtain from (4)

$$(\alpha - \beta)\langle f_{uv}, f_u \rangle = 2\alpha(\log \lambda)_v \langle f_u, f_u \rangle \quad \text{and} \quad (\alpha - \beta)\langle f_{uv}, f_v \rangle = -2\beta(\log \lambda)_u \langle f_v, f_v \rangle,$$

or equivalently, using $(\|f_u\|^2)_v = 2\langle f_{uv}, f_u \rangle$,

$$\frac{\alpha - \beta}{4\alpha}(\log \|f_u\|^2)_v = (\log \lambda)_v \quad \text{and} \quad \frac{\beta - \alpha}{4\beta}(\log \|f_v\|^2)_u = (\log \lambda)_u.$$

Consequently, by integration the two equations we obtain two possibilities for λ . Note that as we integrate the two equations by v and u we have to add functions for both terms which only depend on u and v , respectively. For the sake of simplicity of later expressions we represent these functions with constant factors: $\frac{\beta - \alpha}{2\alpha\beta}g(u)$ and $\frac{\alpha - \beta}{2\alpha\beta}h(v)$. Now, integration yields

$$\log \lambda = \frac{\alpha - \beta}{4\alpha} \log \|f_u\|^2 + \frac{\beta - \alpha}{2\alpha\beta} g(u) \quad \text{and} \quad \log \lambda = \frac{\beta - \alpha}{4\beta} \log \|f_v\|^2 + \frac{\alpha - \beta}{2\alpha\beta} h(v),$$

which after taking the exponential on both sides yields

$$\lambda = (e^{-g(u)}\|f_u\|^\beta)^{\frac{\alpha - \beta}{2\alpha\beta}} \quad \text{and} \quad \lambda = (e^{-h(v)}\|f_v\|^\alpha)^{\frac{\beta - \alpha}{2\alpha\beta}}. \quad (5)$$

Finally, we arrive at two explicit expressions for λ which both must be the same as a necessary condition for λ to exist. The following theorem says that this necessary condition is also sufficient.

Theorem 1. *Let f be a curvature-line net and $\alpha, \beta \in \mathbb{R} \setminus \{0\}$. Then there exists up to translation and scaling a unique curvature-line net f^* and a function $\lambda : \mathbb{R}^2 \rightarrow \mathbb{R}_{>0}$ such that f and f^* are related by a Combescure transformation governed by Equation (3) if and only if*

$$\|f_u\|^\beta \cdot \|f_v\|^\alpha = e^{g(u)+h(v)} \quad (6)$$

for some functions $g(u), h(v)$, or equivalently

$$\partial_u \partial_v \log(\|f_u\|^\beta \cdot \|f_v\|^\alpha) = 0.$$

The net f^* is then of the same type except that α and β are replaced by their reciprocals, i.e., its characterizing equation is

$$\partial_u \partial_v \log(\|f_u^*\|^{\frac{1}{\beta}} \cdot \|f_v^*\|^{\frac{1}{\alpha}}) = 0. \quad (7)$$

Proof. The considerations from above imply that Equation (6) is necessary for the existence of f^* .

On the other hand if Equation (6) holds we can define λ in either way of the two equal representations (5). Inserting λ into Equation (4) implies that the integrability condition for f^* is fulfilled.

As for uniqueness (up to translation and scaling) of f^* for given f , α , and β , we first look at its definition, Equation (3). Only different λ 's can change f^* , so we have to check how much freedom we have for the choice of λ once we are given f , α , and β . Consequently, (5) implies that we have to check the freedom to choose $g(u)$ and $h(v)$. Equation (6) implies that $g(u)$ and $h(v)$ can change only as much as $e^{g(u)+h(v)}$ does not change, i.e., adding to $g(u)$ a constant c and at the same time subtracting the same constant c from $h(v)$, hence $g(u) \rightarrow g(u) + c$ and $h(v) \rightarrow h(v) - c$. This change implies multiplying λ by $e^{-c\frac{\alpha-\beta}{2\alpha\beta}}$ and therefore scaling f^* by $e^{c\frac{\alpha\beta}{\alpha-\beta}}$.

As for Equation (7), i.e., for the lengths of the derivatives of f^* we have:

$$\begin{aligned} \|f_u^*\|^{\frac{1}{\beta}} \cdot \|f_v^*\|^{\frac{1}{\alpha}} &\stackrel{(3)}{=} \left\| \frac{\alpha}{\lambda^2} f_u \right\|^{\frac{1}{\beta}} \cdot \left\| \frac{\beta}{\lambda^2} f_v \right\|^{\frac{1}{\alpha}} \stackrel{(5)}{=} \left\| \frac{\alpha f_u}{(e^{-g(u)} \|f_u\|^\beta)^{\frac{\alpha-\beta}{\alpha\beta}}} \right\|^{\frac{1}{\beta}} \cdot \left\| \frac{\beta f_v}{(e^{-h(v)} \|f_v\|^\alpha)^{\frac{\beta-\alpha}{\alpha\beta}}} \right\|^{\frac{1}{\alpha}} \\ &= |\alpha|^{\frac{1}{\beta}} |\beta|^{\frac{1}{\alpha}} (e^{g(u)\frac{\alpha-\beta}{\beta}+h(v)\frac{\beta-\alpha}{\alpha}})^{\frac{1}{\alpha\beta}} (\|f_u\|^\beta \|f_v\|^\alpha)^{\frac{1}{\alpha\beta}} \stackrel{(6)}{=} |\alpha|^{\frac{1}{\beta}} |\beta|^{\frac{1}{\alpha}} e^{\frac{g(u)}{\beta^2} + \frac{h(v)}{\alpha^2}}. \end{aligned}$$

The last expression is a product of univariate functions that vanishes after $\partial_u \partial_v$. \square

Remark 2. Note that if f fulfills (6) then Theorem 1 implies the existence of f^* which itself fulfills (7) which again by Theorem 1 implies the existence of f^{**} via

$$f_u^{**} = \frac{1}{\alpha \mu^2} f_u^* \quad \text{and} \quad f_v^{**} = \frac{1}{\beta \mu^2} f_v^*, \quad (8)$$

for some function μ . The uniqueness statement of Theorem 1 implies that f^{**} equals f up to scaling and translation since f solves Equation (8) for $\mu = 1/\lambda$.

Remark 3. Note that Equation (6) in the case of $\alpha + \beta = 0$ implies that f is a conformal parametrization (in its “wider” definition, i.e. $f_u \perp f_v$ and $\log(\|f_u\| \|f_v\|)_{uv} = 0$). Therefore, in the case of $\alpha + \beta = 0$, Theorem 1 implies that f is an isothermic net and the special Combescure transformation (3) is the well known Christoffel transformation [5]. We therefore make the following definition.

Definition 4. We call two curvature-line nets f and f^* related by a *Christoffel-type transformation* if they are related by Equation (3).

Remark 5. Note that an appropriate reparametrization \tilde{f} of f , namely $\tilde{f}(u, v) = f(\phi_1(u), \phi_2(v))$ with $\phi_1(u) = \int e^{\frac{-g(u)}{\beta}} du$ and $\phi_2(v) = \int e^{\frac{-h(v)}{\alpha}} dv$ simplifies the general Equation (6) to $\|\tilde{f}_u\|^\beta \cdot \|\tilde{f}_v\|^\alpha = 1$.

2.3 Surfaces from the Gauss map

E. Christoffel [5] constructs minimal surfaces by applying a transformation (which is now called *Christoffel transformation*) to an isothermic parametrization of the unit sphere, the Gauss map.

The Christoffel-type transformations described in Section 2.2 is a generalization of Christoffel's original transformation and includes the Christoffel transformations as special case ($\alpha + \beta = 0$).

With the following theorem we obtain surfaces with a constant ratio of principal curvatures by applying this Christoffel-type transformation (3) to spherical curvature-line nets fulfilling Equation (6).

Theorem 6. Let $\alpha, \beta \in \mathbb{R} \setminus \{0\}$, and let $n : \mathbb{R}^2 \rightarrow S^2$ be a spherical curvature-line parametrization with

$$\partial_u \partial_v \log(\|n_u\|^\beta \cdot \|n_v\|^\alpha) = 0.$$

Then the net $f := n^*$, that we obtain from n by applying the Christoffel-type transformation (3), is a surface with constant ratio of principal curvatures.

Proof. Rodrigues' formula for a curvature-line parametrized surfaces reads

$$-\kappa_1 f_u = n_u \quad \text{and} \quad -\kappa_2 f_v = n_v.$$

Equation (3) on the other hand implies

$$f_u = \frac{\alpha}{\lambda^2} n_u \quad \text{and} \quad f_v = \frac{\beta}{\lambda^2} n_v,$$

and therefore $\alpha \kappa_1 = \beta \kappa_2$. \square

Remark 7. In relative differential geometry the principal curvatures are not measured with respect to the unit sphere as Gauss map but rather with a different sufficiently regular surface instead. However, the curvature theory for surfaces in relative differential geometry is defined in such a way that Rodrigues' formula holds as well. That implies that Theorem 6 still gives us surfaces with constant ratio of principal curvatures in the case where n is not the unit sphere but here in the sense of relative differential geometry.

Remark 8. Denote by $w : \mathbb{C} \rightarrow \mathbb{C}$ the stereographic projection of the Gauss map n of a curvature line net f . Then f is a net with constant ratio of principal curvatures if and only if w fulfills

$$\partial_u \partial_v \log \frac{|w_u|^\beta |w_v|^\alpha}{(1 + |w|^2)^{\alpha + \beta}} = 0.$$

This can easily be verified by pushing forward the metric from the sphere to the plane (metric of the Riemann sphere).

2.4 In the projective model of Möbius geometry

A classical way of studying Möbius geometry in $\mathbb{R}^3 \cup \{\infty\}$ is by lifting its points and spheres to points of the projective space over the Minkowski space $\mathbb{R}^{4,1}$. The *lifting* map has the following form (see e.g. [3]):

$$\begin{aligned} \text{point } p = (p_1, p_2, p_3) \in \mathbb{R}^3 &\longmapsto (p_1, p_2, p_3, \frac{\|f\|^2-1}{2}, \frac{\|f\|^2+1}{2}) \\ \text{point at infinity } \infty &\longmapsto (0, 0, 0, \frac{1}{2}, \frac{1}{2}) \\ \text{sphere with center } c \in \mathbb{R}^3, \text{ radius } r &\longmapsto (c_1, c_2, c_3, \frac{\|c\|^2-r^2-1}{2}, \frac{\|c\|^2-r^2+1}{2}) \\ \text{plane } \langle n, x \rangle = d \text{ with normal vector } n \in S^2 &\longmapsto (n_1, n_2, n_3, d, d) \end{aligned}$$

In Proposition 9 we observe an interesting behaviour of the cross-ratio of 'point-model-representatives' of special Möbius-geometry elements related to our surfaces. For that we need the notion of *principal curvature spheres* which are the two spheres consisting of points x with equations

$$\|x - (f + \frac{1}{\kappa_i} n)\|^2 = \kappa_i^2, \quad i = 1, 2,$$

where f is the surface and n is the unit normal vector at f . In each point of a surface the point, the tangent plane, and the two curvature spheres belong to the same sphere pencil and are thus mapped to four points on a straight line in the projective model. It therefore makes sense to compute their cross-ratio.

Proposition 9. *Let $\hat{f}, \hat{\tau}, \hat{s}_1, \hat{s}_2$ be the lifts to the projective model of Möbius geometry of the surface point f , the tangent plane τ and the two curvature spheres s_1, s_2 . Then, in each point of a surface with constant ratio of principal curvatures the cross-ratio is constant and equals*

$$\text{cr}(\hat{f}, \hat{\tau}, \hat{s}_1, \hat{s}_2) = \frac{\alpha}{\beta}.$$

Proof. For the sake of brevity we write f and n instead of its components in the 5-dimensional vectors of homogeneous coordinates. Then the lifts of f, τ, s_i read

$$\hat{f} = (f, \frac{\|f\|^2 - 1}{2}, \frac{\|f\|^2 + 1}{2}), \quad \hat{\tau} = (n, \langle n, f \rangle, \langle n, f \rangle),$$

$$\hat{s}_i = (f + \kappa_i^{-1} n, \frac{\|f + \kappa_i^{-1} n\|^2 - \kappa_i^{-2} - 1}{2}, \frac{\|f + \kappa_i^{-1} n\|^2 - \kappa_i^{-2} + 1}{2}).$$

Consequently, we can express the curvature sphere lifts as a linear combination of the lifts of the point and the tangent plane (which also confirms that these four elements lie on a line in the projective model):

$$\hat{s}_i = \hat{f} + \frac{1}{\kappa_i} \hat{\tau}.$$

The cross-ratio of four collinear points in homogeneous coordinates $a, b, v_1 a + v_2 b, \mu_1 a + \mu_2 b$ is $\frac{v_1}{v_2} : \frac{\mu_2}{\mu_1}$. With that definition we obtain the cross-ratio

$$\text{cr}(\hat{f}, \hat{\tau}, \hat{s}_1, \hat{s}_2) = \text{cr}(\hat{f}, \hat{\tau}, \hat{f} + \frac{1}{\kappa_1} \hat{\tau}, \hat{f} + \frac{1}{\kappa_2} \hat{\tau}) = \frac{\kappa_2}{\kappa_1} \stackrel{(1)}{=} \frac{\alpha}{\beta},$$

which is what we wanted to show. \square

2.5 Pencils of conjugate nets

In this section we primarily show that surfaces with constant ratio of principal curvatures are characterized by the existence of a particular pencil of conjugate nets. We briefly recalled the notion of conjugate tangents and conjugate nets at the beginning of Section 2.2.

Theorem 10. *Let f denote a net without umbilical and parabolic points. Then the following are equivalent:*

- (i) *The net f has a constant ratio of principal curvatures.*
- (ii) *Let $\{c_t\}$ be a family of curves which intersect the curvature-lines at a constant angle and let $\{d_t\}$ be the family of curves conjugate to $\{c_t\}$ (which exists; see e.g. [7]). Then also the curves $\{d_t\}$ intersect the curvature-lines at a constant angle (Fig. 2 left).*
- (iii) *There is a pencil of conjugate nets (cf. [12]) each of them with a constant intersection angle of parameterlines and such that the parameterlines of any two nets of the pencil intersect each other at a constant angle.*
- (iv) *There exist two conjugate nets on the surface such that the angles between the four tangents to the parameter lines are the same at each point (see Fig. 2 second from left).*

Proof. (i) \Rightarrow (ii): Let $a = (a_1, a_2)$ be a tangent vector of a curve from c_t at some point and expressed in the basis of the principal directions. By assumption each tangent vector encloses a constant angle with the principal directions which implies $a_1 : a_2 = \text{const}$. Since to each tangent line in the tangent plane there is a unique conjugate tangent with direction $b = (b_1, b_2)$ fulfilling $a^\top (\begin{smallmatrix} \kappa_1 & 0 \\ 0 & \kappa_2 \end{smallmatrix}) b = 0$ or equivalently $a^\top (\begin{smallmatrix} \beta & 0 \\ 0 & \alpha \end{smallmatrix}) b = 0$ we also have $b_1 : b_2 = \text{const}$.

(ii) \Rightarrow (iii): For each angle $\varphi \in [0, \pi]$ there is a family of curves $\{c_t^\varphi\}$ on the surface which intersect one family of principal lines at the given angle φ . The pencil we are looking for in (iii) is formed by all such families $\{c_t^\varphi\}$ together with their corresponding families of conjugate curves $\{d_t^\varphi\}$ (which are given by (ii)). φ is the parameter of the pencil. The intersection angles between c_t^φ and d_t^φ can be decomposed as the sum of angles enclosed with the principal directions, which are constant by assumption.

(iv) is just a special case of (iii).

(iv) \Rightarrow (i): The involution of conjugate lines is determined by two pairs of lines and their image lines. Since the two pairs of conjugate tangents given by the assumption are the same in each point, so is the involution of conjugate lines. Therefore, the second fundamental forms in the basis of the principal directions are multiples of each other and consequently $\kappa_1 : \kappa_2 = \text{const}$ everywhere. \square

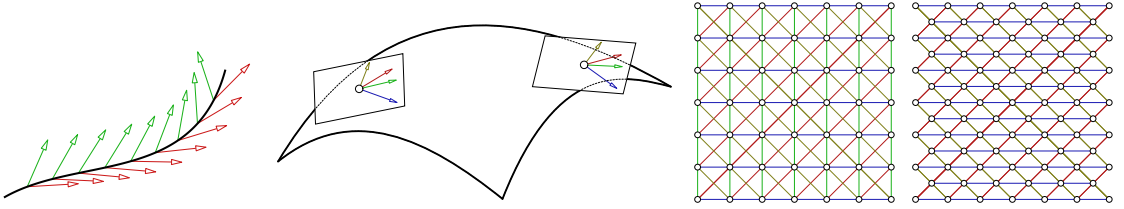


Fig. 2 *Left:* A family of pairs of conjugate directions along a curvature line on a surface with constant ratio of principal directions. If the intersection angle of one family of directions with the curvature line is constant then so is the other. *Second from left:* There exist two conjugate nets on the surface such that the angles between the four tangents to the parameter lines is the same at each point. *Second from right:* A combinatorial view of a very special 4-web. Any three of the families of curves from the 4-web form a hexagonal 3-web. *Right:* A combinatorial view of a hexagonal 3-web.

2.6 Webs of principal and asymptotic lines on isothermic surfaces

An n -web consists of n families of curves on a surface or in the plane such that through each point there is a curve of each family passing through that point and such that any two curves from different families intersect each other at exactly one point (see, e.g., [1]). A very special 4-web in \mathbb{R}^2 is illustrated in Fig. 2 (second from right) consisting of all lines of the form $x = d_1, y = d_2, x + y = d_3, x - y = d_4$, with $d_1, \dots, d_4 \in \mathbb{R}$. A 3-web is called *hexagonal* (see e.g., [1]) if there is a homeomorphism between the surface and the plane such that the curves of the web are mapped to the curves $x = d_1, x + y = d_2, x - y = d_3$, (see Fig. 2 right). Consequently, any three families of the special 4-web from above form a hexagonal 3-web.

Certainly, on any embedded surface patch that can be parametrized we can map the “ideal” planar hexagonal web onto the surface and get a corresponding hexagonal web on the surface which by itself is not particularly worth noticing. However, it becomes significantly more interesting if such a web is determined by the geometry, i.e., for example by the curvature, of the surface.

The following theorem provides a way to find a 4-web of the type illustrated in Fig. 2 (second from right) on an isothermic surface with constant ratio of principal curvatures. The web curves are determined solely by the geometry and curvature of the surface.

Theorem 11. *The curvature-lines and the asymptotic lines of an isothermic surface with constant negative ratio of principal curvatures form a 4-web where any three of the families of curves from the 4-web form a hexagonal 3-web.*

Proof. Let $f(u, v)$ be an isothermic parametrization (i.e., conformal curvature-line parametrization which means $f_u \perp f_v, f_{uv} \perp n, \|f_u\| = \|f_v\|$) of an isothermic surface with constant ratio of principal curvatures. A curve $f(u(t), v(t))$ on that surface is an asymptotic line if

$$\frac{\dot{u}}{\dot{v}} = \pm \frac{\sqrt{|\kappa_2|} \|f_v\|}{\sqrt{|\kappa_1|} \|f_u\|} \quad \text{and therefore} \quad \frac{\dot{u}}{\dot{v}} = \pm \sqrt{\left| \frac{\alpha}{\beta} \right|}.$$

Consequently, asymptotic curves are described in the parameter domain by straight lines with a constant inclination angle with respect to the axes and thus form the “diagonal” families of the 4-web as illustrated in Fig. 2 (second from right). \square

3 Discretization with conjugate nets

In this section we propose a discretization of smooth surfaces with constant ratio of principal curvatures. Our discretization idea is *not* to “wish” for a constant ratio of a *discretization* of the principal curvatures of the mesh (which might be worthwhile studying in a suitable setting). We rather develop a discrete analogue

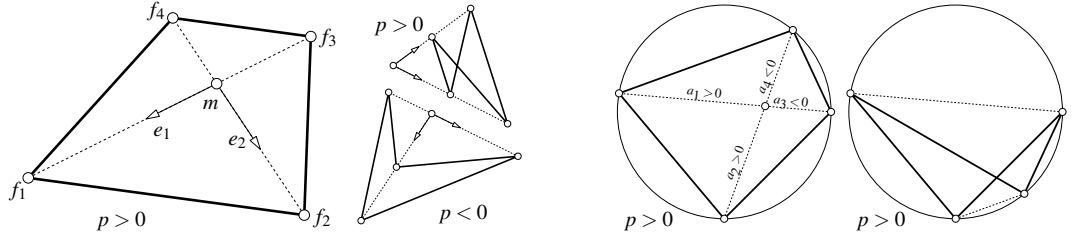


Fig. 3 The vertices of the quadrilateral f are expressed with their oriented distance to the intersection point m of their diagonals. The value $p = a_1a_2a_3a_4$ can be positive or negative depending on whether the vertices lie on the boundary of their convex hull or not. The vertices of circular quadrilaterals (*right*) always lie on the boundary of their convex hull.

of the Christoffel-type transformation (3) for which we show similar properties as in the smooth case (Sec. 2.2). In Section 3.4 we will show Equation (2) for discrete Gaussian and mean curvatures.

In this entire section the objects, i.e., the discrete surfaces, are represented by discrete conjugate nets which are nets with planar quadrilateral faces. Later in Section 4 we will consider a discretization in a different setting namely with asymptotic nets.

3.1 A discrete Christoffel-type transformation

A *discrete conjugate net* \mathcal{M} is a mesh with \mathbb{Z}^2 combinatorics where each face is a planar quadrilateral in \mathbb{R}^3 . Two conjugate nets \mathcal{M} and \mathcal{M}^* (with the same combinatorics) are said to be *parallel* or *related by a discrete Combescure transformation* if corresponding edges are parallel. In that case a transformation from \mathcal{M} to \mathcal{M}^* is called a *discrete Combescure transformation*. To study a particular Combescure transformation we first introduce some notions on quadrilaterals, the basic building block of our meshes.

Let m be the intersection point of the diagonals of a quadrilateral $f = (f_1, f_2, f_3, f_4)$. Then, the vertices of f can be expressed as

$$f_1 = m + a_1 e_1, \quad f_2 = m + a_2 e_2, \quad f_3 = m + a_3 e_1, \quad f_4 = m + a_4 e_2, \quad (9)$$

with $a_i \in \mathbb{R}$, $e_1 \parallel f_1 - f_3$, and $e_2 \parallel f_2 - f_4$ unit normal vectors along the diagonals (see Fig. 3 left).

From now on we assume that the vertices of the quadrilateral lie on the boundary of their convex hull. This ‘convex hull’ assumption thus implies positivity of the product

$$p := a_1a_2a_3a_4 \geq 0.$$

We will frequently use the first forward difference operator which is very commonly denoted by Δ , i.e., $\Delta f_i = f_{i+1} - f_i$.

Proposition 12. *Let f be a quadrilateral and $p = a_1a_2a_3a_4$ be as before. Let further $\alpha, \beta \in \mathbb{R} \setminus \{0\}$ and $\sigma \in \{\pm 1\}$. Then there exists a quadrilateral f^* which is edgewise parallel to f and which has the following edge vectors (indices taken modulo 4)*

$$\Delta f_i^* = \left(\frac{\alpha + \beta}{\sqrt{p}} + \sigma \frac{\alpha - \beta}{a_i a_{i+1}} \right) \Delta f_i, \quad (10)$$

i.e., the discrete (additive) 1-form Δf_i^* is exact.

Proof. To show that the vectors Δf_i^* are edges of an actual quadrilateral f^* (i.e., the exactness of Δf_i^*), we have to show that the four edge vectors add up to zero:

$$\begin{aligned} \sum_{i=1}^4 \Delta f_i^* &= \frac{\alpha + \beta}{\sqrt{p}} \sum_{i=1}^4 \Delta f_i + \sigma(\alpha - \beta) \sum_{i=1}^4 \frac{\Delta f_i}{a_i a_{i+1}} \\ &\stackrel{(9)}{=} 0 + \sigma(\alpha - \beta) \left(\frac{a_2 e_2 - a_1 e_1}{a_1 a_2} + \frac{a_3 e_1 - a_2 e_2}{a_2 a_3} + \dots + \frac{a_1 e_1 - a_4 e_2}{a_4 a_1} \right), \end{aligned}$$

which after canceling is easily seen to be a telescoping sum which adds up to zero. \square

Remark 13. Observe the similarity of Equation (10) to the smooth Christoffel-type transformation (3): the differential is replaced by the difference $\partial_u, \partial_v \leftrightarrow \Delta$ and the ‘order two terms’ in the denominator $\lambda^2 \leftrightarrow a_i a_{i+1}, \sqrt{a_1 a_2 a_3 a_4}$.

Further, notice that transformation (10) for the special case of $\alpha + \beta = 0$ assumes the well known discrete Christoffel transformation for Koenigs nets [4] or at least for one quadrilateral:

$$\Delta f_i^* = \frac{1}{a_i a_{i+1}} \Delta f_i.$$

Recall that also in the smooth setting the case $\alpha + \beta = 0$ characterizes the Christoffel transformation (see Remark 3). Thus the following definition is sensible.

Definition 14. We call two discrete conjugate nets \mathcal{M} and \mathcal{M}^* with the same combinatorics related by a *discrete Christoffel-type transformation* if all corresponding pairs of faces (f, f^*) are related by Equation (10) where we allow for individual scalings of each face.

Note that so far we only applied transformation (10) to one single quadrilateral and it cannot be expected that an entire mesh can be transformed that way. In analogy to the smooth case where we have an integrability condition (Equation (6)) for the existence of a transformed surface f^* , we have to expect a discrete integrability condition in our discrete setting as well. We will provide such a condition by Theorem 21.

A series of transformed quadrilaterals f^* from f using Equation (10) for different $\gamma := \beta : \alpha$ (from $\gamma = 1.5$ to $\gamma = -1.5$ with step size -0.5) is, up to individually different scalings, illustrated by Fig. 4.

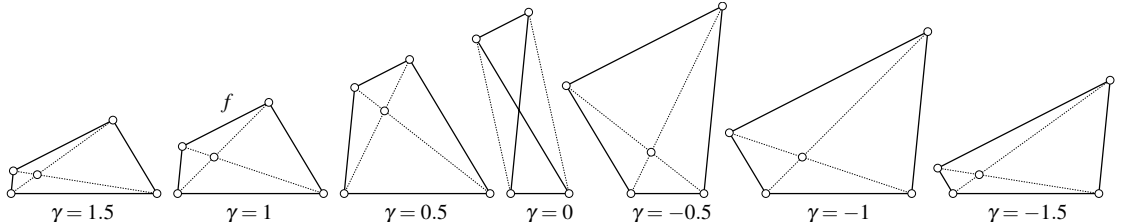


Fig. 4 We construct a sequence of quadrilaterals f^* to a given quadrilateral f using Equation (10) for different $\gamma = \beta : \alpha$ (from $\gamma = 1.5$ to $\gamma = -1.5$ with a step size of -0.5). The quadrilaterals are individually scaled. Note that $f = f^*$ for $\gamma = 1$.

Proposition 15. The directions d_1, d_2 along the diagonals of f^* can be computed from the (unit length) directions e_1, e_2 of the diagonals of f in the following way:

$$d_1 = \frac{\alpha + \beta}{\sqrt{p}} e_1 + \sigma \frac{\alpha - \beta}{a_1 a_3} e_2 \quad \text{and} \quad d_2 = \frac{\alpha + \beta}{\sqrt{p}} e_2 + \sigma \frac{\alpha - \beta}{a_2 a_4} e_1. \quad (11)$$

Proof. To obtain the direction of the diagonal $d_1 \parallel f_3^* - f_1^*$ we add two adjacent edge vectors: $f_3^* - f_2^* + f_2^* - f_1^* = \Delta f_1^* + \Delta f_2^*$ which, using Equation (10), reads

$$f_3^* - f_1^* = \left(\frac{\alpha + \beta}{\sqrt{p}} + \sigma \frac{\alpha - \beta}{a_1 a_2} \right) (f_2 - f_1) + \left(\frac{\alpha + \beta}{\sqrt{p}} + \sigma \frac{\alpha - \beta}{a_2 a_3} \right) (f_3 - f_2).$$

Making use of the notation of (9) we collect the coefficients of e_1 and e_2 and get

$$f_3^* - f_1^* = \left[\frac{\alpha + \beta}{\sqrt{p}} (a_3 - a_1) \right] e_1 + \sigma \left[\frac{\alpha - \beta}{a_1 a_3} (a_3 - a_1) \right] e_2, \quad (12)$$

which is $(a_3 - a_1)$ times the claimed direction vector. Analogously the direction of the other diagonal. \square

In analogy to Remark 2, we will determine f^{**} for the discrete case in Proposition 18 as well. To that end, let us represent the vertices of f^* in the same way as f (i.e., in analogy to (9)):

$$f_1^* = m^* + a_1^* e_1^*, \quad f_2^* = m^* + a_2^* e_2^*, \quad f_3^* = m^* + a_3^* e_1^*, \quad f_4^* = m^* + a_4^* e_2^*,$$

where $e_1^* \parallel f_1^* - f_3^*$ and $e_2^* \parallel f_2^* - f_4^*$. Note that also $e_1^* \parallel d_1$ and $e_2^* \parallel d_2$.

Lemma 16. *For the oriented distances a_i^* from m^* to f_i^* we get*

$$a_1^* = A_1^* \|d_1\|, \quad a_2^* = A_2^* \|d_2\|, \quad a_3^* = A_3^* \|d_1\|, \quad a_4^* = A_4^* \|d_2\|,$$

with

$$A_i^* := \frac{1}{4\alpha\beta} [a_i(\alpha + \beta)^2 + a_{i+2}(\alpha - \beta)^2 + \sigma \left(\frac{\sqrt{p}}{a_{i+1}} + \frac{\sqrt{p}}{a_{i+3}} \right) (\alpha^2 - \beta^2)].$$

Proof. We have

$$\begin{aligned} & \left(\frac{\alpha + \beta}{\sqrt{p}} + \sigma \frac{\alpha - \beta}{a_1 a_2} \right) (a_2 e_2 - a_1 e_1) \stackrel{(10)}{=} \Delta f_1^* = (m^* + a_2^* e_2^*) - (m^* + a_1^* e_1^*) \\ &= A_2^* \|d_2\| \frac{d_2}{\|d_2\|} - A_1^* \|d_1\| \frac{d_1}{\|d_1\|} \stackrel{(11)}{=} A_2^* \left(\frac{\alpha + \beta}{\sqrt{p}} e_2 + \sigma \frac{\alpha - \beta}{a_2 a_4} e_1 \right) - A_1^* \left(\frac{\alpha + \beta}{\sqrt{p}} e_1 + \sigma \frac{\alpha - \beta}{a_1 a_3} e_2 \right), \end{aligned}$$

which leads to the system

$$\begin{pmatrix} -\frac{\alpha + \beta}{\sqrt{p}} & \sigma \frac{\alpha - \beta}{a_2 a_4} \\ -\sigma \frac{\alpha - \beta}{a_1 a_3} & \frac{\alpha + \beta}{\sqrt{p}} \end{pmatrix} \begin{pmatrix} A_1^* \\ A_2^* \end{pmatrix} = \begin{pmatrix} -a_1 \left(\frac{\alpha + \beta}{\sqrt{p}} + \sigma \frac{\alpha - \beta}{a_1 a_2} \right) \\ a_2 \left(\frac{\alpha + \beta}{\sqrt{p}} + \sigma \frac{\alpha - \beta}{a_1 a_3} \right) \end{pmatrix},$$

whose solution gives us A_1^* and A_2^* , and analogously we obtain A_3^* and A_4^* . \square

Lemma 17. *We have the identity*

$$\frac{A_1^* A_3^*}{a_1 a_3} = \frac{A_2^* A_4^*}{a_2 a_4}.$$

Proof. Using $p = a_1 a_2 a_3 a_4$ and $\sigma^2 = 1$, we compute

$$\begin{aligned} \frac{A_1^* A_3^*}{a_1 a_3} &= \frac{1}{16\alpha^2\beta^2} [(\alpha + \beta)^4 + (\alpha - \beta)^4 + 2(\alpha^2 - \beta^2)^2 + \left(\frac{a_1}{a_3} + \frac{a_3}{a_1} + \frac{a_2}{a_4} + \frac{a_4}{a_2} \right) (\alpha^2 - \beta^2)^2 \\ &\quad + 2\sigma\sqrt{p} \left(\frac{1}{a_1} + \frac{1}{a_3} \right) \left(\frac{1}{a_2} + \frac{1}{a_4} \right) (\alpha^4 - \beta^4)]. \end{aligned}$$

The right hand side of the last equation is symmetric when exchanging $(a_1, a_3) \leftrightarrow (a_2, a_4)$. Consequently, $\frac{A_2^* A_4^*}{a_2 a_4}$ computes to the same which is what we wanted to show. \square

The following proposition is the discrete analogue to Remark 2, i.e., we show that as we apply the $*$ -transformation twice we obtain the original quadrilateral up to scaling and translation.

Proposition 18. f^{**} is similar to f , and

$$\Delta f_i^{**} = \left(\frac{\frac{1}{\alpha} + \frac{1}{\beta}}{\sqrt{p^*}} + \sigma \frac{\frac{1}{\alpha} - \frac{1}{\beta}}{a_i^* a_{i+1}^*} \right) \Delta f_i^*,$$

which corresponds to transformation (10) if we replace (α, β) by $(\frac{1}{\alpha}, \frac{1}{\beta})$.

Proof. From the definition of the $*$ -construction, Equation (10), we immediately get that the edges of f and f^{**} are parallel. Consequently, f and f^{**} are similar if and only if the diagonals are parallel too. It is sufficient to show $f_3^{**} - f_1^{**} \parallel f_3 - f_1$ or equivalently $f_3^{**} - f_1^{**} \parallel e_1$. Since we are only interested in the direction of the diagonal and not in its length we just compute its linear span:

$$\begin{aligned} \text{sp}(f_3^{**} - f_1^{**}) &= \text{sp} d_1^* \stackrel{(11)^*}{=} \text{sp} \left(\frac{\frac{1}{\alpha} + \frac{1}{\beta}}{\sqrt{p^*}} e_1^* + \sigma \frac{\frac{1}{\alpha} - \frac{1}{\beta}}{a_1^* a_3^*} e_2^* \right) = \text{sp} \left(\frac{\alpha + \beta}{\sqrt{p^*} \|d_1\|} e_1 - \sigma \frac{\alpha - \beta}{a_1^* a_3^*} \frac{d_2}{\|d_2\|} \right) \\ &= \text{sp} \left(\frac{\alpha + \beta}{\sqrt{p^*} \|d_1\|} \left(\frac{\alpha + \beta}{\sqrt{p}} e_1 + \sigma \frac{\alpha - \beta}{a_1 a_3} e_2 \right) - \sigma \frac{\alpha - \beta}{a_1^* a_3^* \|d_2\|} \left(\frac{\alpha + \beta}{\sqrt{p}} e_2 + \sigma \frac{\alpha - \beta}{a_2 a_4} e_1 \right) \right) \\ &= \text{sp} \left(\dots e_1 + \left(\sigma \frac{\alpha^2 - \beta^2}{\sqrt{p^*} \|d_1\| a_1 a_3} - \sigma \frac{\alpha^2 - \beta^2}{\sqrt{p} \|d_2\| a_1^* a_3^*} \right) e_2 \right). \end{aligned}$$

Consequently, $f_3^{**} - f_1^{**}$ is parallel to e_1 if and only if

$$\frac{1}{\sqrt{p^*} \|d_1\| a_1 a_3} - \frac{1}{\sqrt{p} \|d_2\| a_1^* a_3^*} = 0, \quad \text{and}$$

which, using Lemma 16, is equivalent to

$$\frac{\sqrt{A_1^* \|d_1\| A_2^* \|d_2\| A_3^* \|d_1\| A_4^* \|d_2\|} \|d_1\|}{\sqrt{a_1 a_2 a_3 a_4}} = \frac{\|d_2\| A_1^* \|d_1\| A_3^* \|d_1\|}{a_1 a_3},$$

and further, equivalent to

$$\sqrt{\frac{A_1^* A_2^* A_3^* A_4^*}{a_1 a_2 a_3 a_4}} = \frac{A_1^* A_3^*}{a_1 a_3}.$$

Now, Lemma 17 implies that the last equation is true which concludes the proof. \square

3.2 Characterization of nets \mathcal{M} which allow for Christoffel-type transformations

In this section we discuss the conditions for a net \mathcal{M} such that there exists a Christoffel-type transform \mathcal{M}^* (see Definition 14). We know how to construct a quadrilateral f^* from a given quadrilateral f via Equation (10) but we do not know if all transformed quadrilaterals will fit together and form a mesh. We allow for different scalings of each individual transformed face f^* , but for example, as we apply (10) to the faces around a vertex, we have no guarantee that the transformed faces close up, as we go around, and consequently generate a net.

In the following two sections we derive a discrete anaolgue of the smooth integrability condition (6). We describe an algebraic and a geometric characterization of such nets \mathcal{M} which allow for a discrete Christoffel-type transformation.

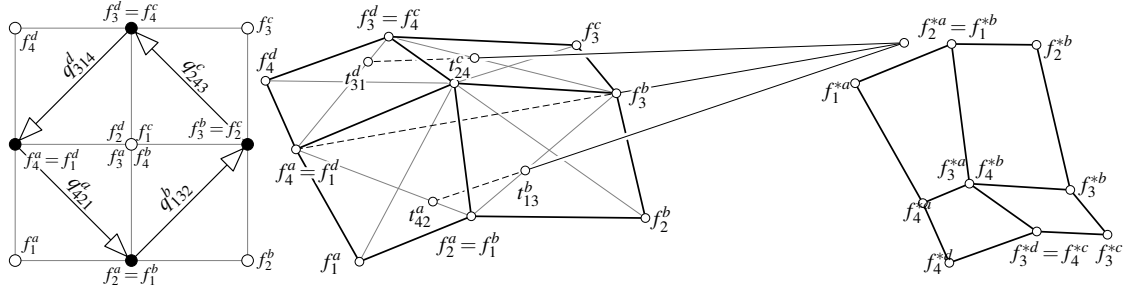


Fig. 5 Left: Four quadrilaterals around a white vertex. The values q are defined via Equation (13) on the illustrated oriented diagonals. Center: Illustration of the geometric condition on \mathcal{M} for the existence of a discrete Christoffel-type transform \mathcal{M}^* (here for $\alpha + 2\beta = 0$): The three lines $(t_{42}^a t_{13}^b)$, $(t_{24}^c t_{31}^d)$ and $(f_4^a f_3^b)$ intersect in one point if and only if the Christoffel-type transform \mathcal{M}^* (right) exists.

3.2.1 Algebraic characterization

In this section we will characterize meshes \mathcal{M} which allow for a discrete Christoffel-type transformation (10). This condition is local, and it is defined on the four faces around a vertex. We call the four faces ‘ a, b, c, d ’, and denote the oriented distances from the intersection point of the diagonals of the four quadrilaterals accordingly by a_i, b_i, c_i, d_i in counter clockwise order.

On each of the oriented diagonals of our oriented nets we define a real valued function q . Its value on the oriented diagonal between i and k in the oriented face ‘ $a = (i, j, k, l)$ ’ is (recall the notion $p = a_1 a_2 a_3 a_4$ and also see Fig. 5 left):

$$q_{ikj}^a(\alpha, \beta) := \frac{\sqrt{p}(\alpha + \beta) + \sigma a_k a_j (\alpha - \beta)}{\sqrt{p}(\alpha + \beta) + \sigma a_i a_l (\alpha - \beta)}. \quad (13)$$

Consequently, the value of q of the same diagonal but reversely oriented is $q_{kil}^a(\alpha, \beta) = \frac{\sqrt{p}(\alpha + \beta) + \sigma a_i a_l (\alpha - \beta)}{\sqrt{p}(\alpha + \beta) + \sigma a_k a_l (\alpha - \beta)}$. The relation between the two orientations is given by

Lemma 19. *In every quadrilateral we have*

$$q_{ikj}^a(\alpha, \beta) = \frac{a_k}{a_i} q_{kil}^a(\alpha, -\beta). \quad (14)$$

Proof. We start with the right hand side (recall $\sigma^2 = 1$)

$$\begin{aligned} \frac{a_k}{a_i} q_{kil}^a(\alpha, -\beta) &= \frac{a_k}{a_i} \cdot \frac{\sqrt{p}(\alpha - \beta) + \sigma a_i a_l (\alpha + \beta)}{\sqrt{p}(\alpha - \beta) + \sigma a_k a_l (\alpha + \beta)} \cdot \frac{\sqrt{p}}{\sqrt{p}} \cdot \frac{\sigma}{\sigma} \\ &= \frac{a_k}{a_i} \cdot \frac{\sigma a_i a_j a_k a_l (\alpha - \beta) + \sqrt{p} a_i a_l (\alpha + \beta)}{\sigma a_i a_j a_k a_l (\alpha - \beta) + \sqrt{p} a_k a_l (\alpha + \beta)} = q_{ikj}^a(\alpha, \beta). \end{aligned} \quad \square$$

Remark 20. In the special case of Koenigs nets, the function q simplifies to the discrete multiplicative 1-form q_{ik}

$$q_{ik} := q_{ikj}^a(\alpha, -\alpha) = \frac{a_k}{a_i} = \frac{1}{q_{kil}^a(\alpha, -\alpha)} = \frac{1}{q_{ik}}$$

as $\alpha + \beta = 0$ (cf. [3] for the discrete multiplicative 1-form on Koenigs nets). Note that our more general setting we have the property $q_{ikj}^a(\alpha, \beta) \neq 1/q_{kil}^a(\alpha, \beta)$ that we have for Koenigs nets.

With the following theorem we show how q can be used to locally characterize nets \mathcal{M} which can be transformed to a mesh \mathcal{M}^* via the Christoffel-type transformation (10).

Theorem 21. *There is a discrete Christoffel-type transform \mathcal{M}^* of a quadrilateral net \mathcal{M} if and only if around each vertex of \mathcal{M} the product of the corresponding q 's multiplies to 1 (for the notations see also Fig. 5 left):*

$$q_{421}^a(\alpha, \beta) \cdot q_{132}^b(\alpha, \beta) \cdot q_{243}^c(\alpha, \beta) \cdot q_{314}^d(\alpha, \beta) = 1, \quad (15)$$

or equivalently

$$q_{243}^a(\alpha, \beta) \cdot q_{314}^b(\alpha, \beta) \cdot q_{421}^c(\alpha, \beta) \cdot q_{132}^d(\alpha, \beta) = \frac{a_4 b_1 c_2 d_3}{a_2 b_3 c_4 d_1}.$$

Proof. Let us denote by $k_{ij}^a, k_{ij}^b, k_{ij}^c, k_{ij}^d$ the factors of Δf_i in Equation (10), i.e., for example

$$k_{23}^b = \left(\frac{\alpha + \beta}{\sqrt{p}} + \sigma \frac{\alpha - \beta}{b_2 b_3} \right),$$

such that $\Delta f_2^* = k_{23}^b \Delta f_2$. Recall, for the Christoffel-type transformation $\mathcal{M} \rightarrow \mathcal{M}^*$ we allow for individual scalings of faces. Consequently, the four transformed quadrilaterals around a common central vertex fit together in \mathcal{M}^* if and only if there exist four scaling factors $r^a, r^b, r^c, r^d \in \mathbb{R} \setminus \{0\}$ such that

$$r^a k_{23}^a = r^b k_{14}^b, \quad r^b k_{34}^b = r^c k_{12}^c, \quad r^c k_{14}^c = r^d k_{23}^d, \quad r^d k_{12}^d = r^a k_{34}^a.$$

The existence of these scaling factors is equivalent to the equation

$$1 = \frac{r^a}{r^b} \cdot \frac{r^b}{r^c} \cdot \frac{r^c}{r^d} \cdot \frac{r^d}{r^a} = \frac{k_{14}^b}{k_{23}^a} \cdot \frac{k_{12}^c}{k_{34}^b} \cdot \frac{k_{23}^d}{k_{14}^c} \cdot \frac{k_{34}^a}{k_{12}^d}.$$

Rearranging the last term yields

$$1 = \frac{k_{34}^a}{k_{23}^a} \cdot \frac{k_{14}^b}{k_{34}^b} \cdot \frac{k_{12}^c}{k_{14}^c} \cdot \frac{k_{23}^d}{k_{12}^d}. \quad (16)$$

Now for these ratios we have, for example for 'a':

$$\frac{k_{34}^a}{k_{23}^a} = \frac{\frac{\alpha+\beta}{\sqrt{p}} + \sigma \frac{\alpha-\beta}{a_3 a_4}}{\frac{\alpha+\beta}{\sqrt{p}} + \sigma \frac{\alpha-\beta}{a_2 a_3}} = \frac{\sqrt{p}(\alpha+\beta) + \sigma a_1 a_2 (\alpha-\beta)}{\sqrt{p}(\alpha+\beta) + \sigma a_1 a_4 (\alpha-\beta)} = q_{421}^a(\alpha, \beta).$$

Consequently, using (13) and (16) we get

$$1 = q_{421}^a(\alpha, \beta) \cdot q_{132}^b(\alpha, \beta) \cdot q_{243}^c(\alpha, \beta) \cdot q_{314}^d(\alpha, \beta),$$

which implies the equivalence of the constructability of \mathcal{M} and the claimed property of q . The second equation of the theorem follows immediately from Equation (14). \square

From Proposition 18 we know that f^{**} is similar to f , i.e., the transform \mathcal{M}^{**} of the transform \mathcal{M}^* is similar to the original \mathcal{M} . In particular we obtain that \mathcal{M}^* fulfills the same type of compatibility condition as \mathcal{M} in Theorem 21 except that (α, β) is replaced by $(1/\alpha, 1/\beta)$:

Corollary 22. *The transformed net \mathcal{M}^* fulfills*

$$q_{421}^a(\alpha^{-1}, \beta^{-1}) \cdot q_{132}^b(\alpha^{-1}, \beta^{-1}) \cdot q_{243}^c(\alpha^{-1}, \beta^{-1}) \cdot q_{314}^d(\alpha^{-1}, \beta^{-1}) = 1.$$

3.2.2 Geometric characterization

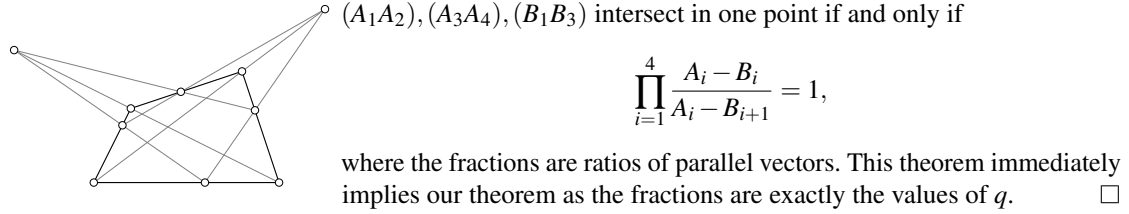
In analogy to the characterization of discrete Koenigs nets in [4], the algebraic characterization, given by Theorem 21, has a similar incidence geometric interpretation. For that consider the quadrilateral $a = (f_1^a, f_2^a, f_3^a, f_4^a)$ with the value q_{ikl}^a from (13) defined on the oriented diagonal $ik = f_i^a - f_k^a$. The affine combination

$$t_{ik}^a = \frac{1}{1 - q_{ikl}^a} f_i - \frac{q_{ikl}^a}{1 - q_{ikl}^a} f_k \quad (17)$$

determines a point on the diagonal. We denote again the four faces around a vertex by a, b, c, d . For an illustration of the notation see Fig. 5 (center and right).

Theorem 23. *Let \mathcal{M} be a planar quadrilateral net. Then the three lines $(t_{42}^a t_{13}^b)$, $(t_{24}^c t_{31}^d)$ and $(f_4^a f_3^b)$ intersect in one point if and only if there exists a discrete Christoffel-type transform \mathcal{M}^* of \mathcal{M} (see Fig. 5 center and right). And the analogous property holds with the three lines $(t_{42}^a t_{31}^d)$, $(t_{13}^b t_{24}^c)$ and $(f_2^a f_3^d)$. Note, that $f_2^a = f_1^b$ etc.*

Proof. A generalization of Ceva's theorem to a 4-gon states [10, Prop. 2.6]: For a (possibly non-planar) quadrilateral B_1, \dots, B_4 with points A_1, \dots, A_4 on its edges, i.e., $A_i \in (B_i B_{i+1})$, we have the following equivalence:



3.3 Circular nets with constant ratio of principal curvatures

A *circular* net is a net where all faces have a circumcircle, meaning that all its vertices lie on a circle. In the previous section we were considering \mathcal{M} as the Gauss image of a net \mathcal{M}^* with constant ratio of principal curvatures. It is thus a sensible assumption for the net \mathcal{M} to be ‘spherical’. One common way of interpreting a net to be spherical is that all its vertices are inscribed in a sphere, which then is a circular net (since all faces are planar). Therefore all spherical nets (in that sense) and all their parallel nets are circular. For these nets the formulas for the discrete Christoffel-type transformation (10) as well as for the diagonals simplify. The reason for this simplification is the “power of a point theorem” which implies

$$a_1 a_3 = a_2 a_4 \quad (18)$$

for the values a_i defined by (9).

Proposition 24. *Let f be a circular quadrilateral. Then, up to scalings, Equation (10) transforms the edges like*

$$\Delta f_i^* = ((\alpha + \beta) + \varepsilon \sigma(\alpha - \beta) \frac{a_{i+3}}{a_i}) \Delta f_i,$$

whereas the directions of the diagonals transform like

$$e_1 \rightarrow d_1 = (\alpha + \beta) e_1 + \varepsilon \sigma(\alpha - \beta) e_2 \quad \text{and} \quad e_2 \rightarrow d_2 = (\alpha - \beta) e_1 + \varepsilon \sigma(\alpha + \beta) e_2, \quad (19)$$

with $\varepsilon = 1$ if f is self-intersecting and $\varepsilon = -1$ otherwise (see Fig. 3 right). Note that the transformation of the diagonals does not depend on the a_i 's.

Proof. For the edges we multiply the vector (10) by \sqrt{p} and obtain for the factor of $\sigma(\alpha - \beta)$

$$\begin{aligned} \frac{\sqrt{p}}{a_i a_{i+1}} &= \operatorname{sgn}(a_i a_{i+1}) \frac{\sqrt{a_1 a_2 a_3 a_4}}{\sqrt{a_i^2 a_{i+1}^2}} = \operatorname{sgn}(a_i a_{i+1}) \sqrt{\frac{a_{i+2} a_{i+3}}{a_i a_{i+1}}} \\ &\stackrel{(*)}{=} \operatorname{sgn}(a_i a_{i+1}) \sqrt{\frac{a_{i+3}^2}{a_i^2}} = \operatorname{sgn}(a_i^2 a_{i+1} a_{i+3}) \frac{a_{i+3}}{a_i}, \end{aligned}$$

where we use Equation (18) in the form $a_i a_{i+2} = a_{i+1} a_{i+3}$ at (*). Observe $\varepsilon = \operatorname{sgn}(a_{i+1} a_{i+3})$ (cf. Fig. 3 right). As for the diagonals, we multiply the first vector of Equation (11) by \sqrt{p} and obtain for the factor of $\sigma(\alpha - \beta) e_2$

$$\frac{\sqrt{p}}{a_1 a_3} = \operatorname{sgn}(a_1 a_3) \frac{\sqrt{a_1 a_2 a_3 a_4}}{\sqrt{a_1^2 a_3^2}} = \operatorname{sgn}(a_1 a_3) \sqrt{\frac{a_2 a_4}{a_1 a_3}} \stackrel{(18)}{=} \operatorname{sgn}(a_1 a_3) = \varepsilon,$$

see also Fig. 3 right. \square

Remark 25. In the case of a circular quadrilateral, f^* can be easily constructed from f by placing the first edge $f_1^* - f_2^* \parallel f_1 - f_2$ and then drawing the diagonals parallel to the vectors as described by Proposition 24, which both enclose the same angle to e_i (see Fig. 6 right). Then parallel translate the remaining edges and intersect with the existing lines as indicated by Fig. 6 (right).

3.4 Discrete Gaussian and mean curvature

In analogy to the smooth setting we will connect the discrete Christoffel-type transformation to discrete surfaces with constant ratio of principal curvatures.

As mentioned before we will obtain discrete surfaces with constant ratio of principal curvatures not by considering discrete principal curvatures (like e.g. from the ‘discrete Rodrigues’ formula’ $-\kappa_{ij}(f_i^* - f_j^*) = (f_i - f_j)$ in [2]). Instead, we obtain a discrete version of Equation (2) for nets \mathcal{M}^* which are Christoffel-type transforms of nets \mathcal{M} , which we will consider as their Gauss map. It turns out that the discrete Gaussian and mean curvature which are derived from Steiner’s formula for parallel meshes [2] fulfill a discrete analogue of Equation (2), as we will see in the following.

This curvature theory [2] provides a discrete Gaussian and a discrete mean curvature notion that is defined on the pairs of corresponding faces (f, f^*) of a polyhedral surface \mathcal{M}^* with respect to an edgewise parallel surface \mathcal{M} , the Gauss map. Both meshes, \mathcal{M}^* and \mathcal{M} must have the same combinatorics.

For a pair of corresponding faces $f^* = (f_1^*, \dots, f_n^*) \in \mathcal{M}^*$ and $f = (f_1, \dots, f_n) \in \mathcal{M}$ the curvatures are defined as (cf. [2])

$$K_{f,f^*} = \frac{\operatorname{area}(f)}{\operatorname{area}(f^*)}, \quad H_{f,f^*} = -\frac{\operatorname{area}(f^*, f)}{\operatorname{area}(f^*)},$$

where $\operatorname{area}(f^*, f) = \frac{1}{4} \sum_{i=1}^n [\det(f_i^*, f_{i+1}, N) + \det(f_i, f_{i+1}^*, N)]$ is the *mixed area* of two edgewise parallel polygons and where N is a unit normal vector of the plane containing f^* . Note that $\operatorname{area}(f) = \operatorname{area}(f, f)$ is the oriented area of the polygon f , and that $\operatorname{area}(f^*, f)$ is a symmetric bilinear form on the vector space of parallel n -gons (cf. [2, 15]).

The characterizing property in our discretization is a discretized version of Equation (2). We obtain it by simply replacing the smooth Gaussian and mean curvature by their discrete counterparts:

$$4\alpha\beta H_{f,f^*}^2 - (\alpha + \beta)^2 K_{f,f^*} = 0. \tag{20}$$

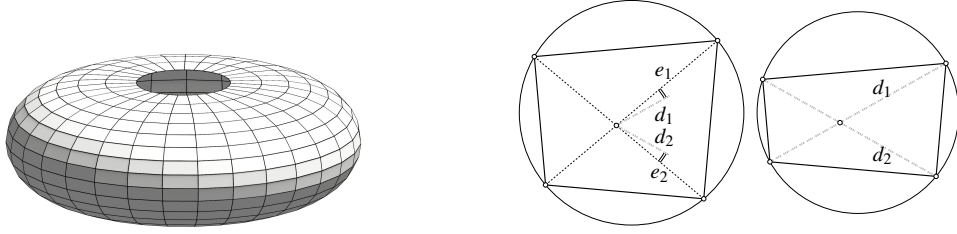


Fig. 6 *Left:* A discrete surface of revolution with constant ratio of principal curvature $\kappa_1/\kappa_2 = 4$. The faces are planar (even circular) quadrilaterals. *Right:* The discrete Christoffel-type transformation in the circular case for $\alpha = 2, \beta = 3$. The directions d_1, d_2 of the new diagonals deviate from the old directions e_1, e_2 by the same angle.

Definition 26. We call a mesh or net \mathcal{M}^* a *net with constant ratio of principal curvatures* with respect to its Gauss map \mathcal{M} if each corresponding pair of faces (f, f^*) fulfills Equation (20). The *ratio* is then defined to be $\alpha : \beta$.

Remark 27. Note that the discrete curvature theory [2] is defined for general polyhedral meshes (not just with quadrilateral faces). Consequently, Definition 26 for discrete surfaces with constant ratio of principal curvatures can be understood in this generality. However, we will restrict ourselves in the present paper to the quadrilateral case.

Notice the symmetry of Equation (20): If a pair of edgewise parallel polygons (f, f^*) fulfills Equation (20) then also the reversed pair (f^*, f) fulfills the same equation for the same α and β . It means that also \mathcal{M} is a mesh with constant ratio of principal curvatures with respect to the “Gauss map” \mathcal{M}^* . Observing

$$H_{f,vf^*} = \frac{1}{v} H_{f,f^*}, \quad K_{f,vf^*} = \frac{1}{v^2} K_{f,f^*}, \quad H_{\mu f,f^*} = \mu H_{f,f^*}, \quad K_{\mu f,f^*} = \mu^2 K_{f,f^*},$$

we see that if Equation (20) holds for the pair (f, f^*) then it also holds for the pair $(vf^*, \mu f)$, with $v, \mu \in \mathbb{R} \setminus \{0\}$. Further, Equation (20) is invariant under independent translations of f^* and f . Consequently the property of being a mesh with constant ratio of principal curvatures is invariant under similarities of the form $f^* \mapsto vf^* + a$, with $v \in \mathbb{R} \setminus \{0\}, R \in O(3), a \in \mathbb{R}^3$, if the Gauss map \mathcal{M} is rotated in the same way, i.e., $f \mapsto Rf$.

Moreover, the oriented area and the oriented mixed area are multiplied by $\det(A)$ as we apply an affine transformation $x \mapsto Ax + a$ (with $A \in \text{GL}_3(\mathbb{R}), a \in \mathbb{R}^3$) to f^* and f simultaneously. Consequently, we obtain the following proposition.

Proposition 28. Let $F(x) := Ax + a$ with $A \in \text{GL}_3(\mathbb{R}), a \in \mathbb{R}^3$ and $v \in \mathbb{R} \setminus \{0\}$.

- (i) If \mathcal{M}^* is a net with constant ratio of principal curvatures with respect to its Gauss map \mathcal{M} , then so is $vF(\mathcal{M}^*)$ with respect to $F(\mathcal{M})$.
- (ii) The property of being the Gauss map of a net with constant ratio of principal curvatures is affinely invariant.

Furthermore, applying an isometry does not change the oriented area and the oriented mixed area up to sign, which implies that we can do computations with these ‘areas’ in the plane and omit the normal vector N in the formulas.

The following theorem shows that the construction from Proposition 12 yields a pair of edgewise parallel faces (f, f^*) which fulfills Equation (2). It therefore provides a transformation of a discrete Gauss map \mathcal{M} to a discrete surface \mathcal{M}^* with constant ratio of principal curvatures, assuming such a mesh \mathcal{M}^* (with respect to \mathcal{M}) exists. The characterization of meshes \mathcal{M} such that \mathcal{M}^* is a net with constant ratio of principal curvatures with respect to \mathcal{M} , is precisely the same as for the existence of a Christoffel-type transform \mathcal{M}^* (Theorems 21 and 23). That will become clear after the next theorem which says that both \mathcal{M}^* ’s are actually the same.

Theorem 29. Let \mathcal{M}^* be a discrete Christoffel-type transform of \mathcal{M} . Then \mathcal{M}^* is a mesh with constant ratio of principal curvatures.

Proof. We will show Equation (20) for a pair of parallel polygons (f, f^*) , related via Equation (10). Its ingredients are H_{f,f^*} and K_{f,f^*} which are composed of areas and mixed areas. To simplify the computation we take advantage of the formula for the mixed area that uses only ‘half’ of its indices (which can be found in [15]):

$$2 \text{area}(f^*, f) = \sum_{i \in \{1, 3, \dots, n-1\}} \det(f_i^*, f_{i+1} - f_{i-1}).$$

In our case, $n = 4$, it reads

$$2 \text{area}(f^*, f) = \det(f_1^*, f_2 - f_4) + \det(f_3^*, f_4 - f_2) = \det(f_1^* - f_3^*, f_2 - f_4),$$

and consequently,

$$2 \text{area}(f^*) = \det(f_1^* - f_3^*, f_2^* - f_4^*), \quad \text{and} \quad 2 \text{area}(f) = \det(f_1 - f_3, f_2 - f_4).$$

Inserting expressions in terms of the basis e_1, e_2 , i.e., Equations (9) and (12), yields

$$\begin{aligned} 2 \text{area}(f^*, f) &= \det \left((a_1 - a_3) \left(\frac{\alpha + \beta}{\sqrt{p}} e_1 + \sigma \frac{\alpha - \beta}{a_1 a_3} e_2 \right), a_2 e_2 - a_4 e_2 \right) \\ &= (a_1 - a_3)(a_2 - a_4) \frac{\alpha + \beta}{\sqrt{p}} \det(e_1, e_2), \end{aligned}$$

and (recall $p = a_1 a_2 a_3 a_4$ and $\sigma^2 = 1$)

$$\begin{aligned} 2 \text{area}(f^*) &= (a_1 - a_3)(a_2 - a_4) \det \left(\frac{\alpha + \beta}{\sqrt{p}} e_1 + \sigma \frac{\alpha - \beta}{a_1 a_3} e_2, \frac{\alpha + \beta}{\sqrt{p}} e_2 + \sigma \frac{\alpha - \beta}{a_1 a_3} e_1 \right) \\ &= (a_1 - a_3)(a_2 - a_4) \left(\frac{(\alpha + \beta)^2}{p} - \frac{\sigma^2 (\alpha - \beta)^2}{p} \right) \det(e_1, e_2), \\ &= \frac{4\alpha\beta}{p} (a_1 - a_3)(a_2 - a_4) \det(e_1, e_2), \end{aligned} \tag{21}$$

and further

$$2 \text{area}(f) = \det(a_1 e_1 - a_3 e_1, a_2 e_2 - a_4 e_2) = (a_1 - a_3)(a_2 - a_4) \det(e_1, e_2).$$

Finally, we show our main equation

$$4\alpha\beta H_{f,f^*}^2 - (\alpha + \beta)^2 K_{f,f^*} = 0$$

which is equivalent to

$$4\alpha\beta \text{area}(f^*, f)^2 - (\alpha + \beta)^2 \text{area}(f^*) \text{area}(f) = 0,$$

simply by inserting our just prepared expressions. \square

So the discrete Christoffel-type transformation, transforms a spherical net \mathcal{M} which fulfills the discrete integrability condition (15) around each face into a mesh \mathcal{M}^* with constant ratio of principal curvatures (in analogy to Theorem (6)).

3.5 Special cases $\alpha - \beta = 0$, $\alpha + \beta = 0$, $\alpha\beta = 0$

We consider three different special cases where the ratio of the principal curvatures expressed in α and β takes three special values.

$\alpha - \beta = 0$: This case is equivalent to the condition $H_{f,f^*}^2 - K_{f,f^*} = 0$ and corresponds, at smooth surfaces, to $\kappa_1 = \kappa_2$, i.e., every point is an umbilic, thus a plane or a sphere. This is reflected in the discrete setting by the trivial transformation $\Delta f_i \xrightarrow{\alpha=\beta} \Delta f_i^* = \frac{2\alpha}{\sqrt{p}} \Delta f_i$ (cf. Equation (10)), which is a similarity. Consequently, if \mathcal{M} is a ‘spherical’ mesh, then so is the transformed mesh \mathcal{M}^* . Corresponding diagonals of f^* and f are parallel (see Equation (11)).

$\alpha + \beta = 0$: This case is very well studied and we have considered this case as a special case several times before. It is equivalent to $H_{f,f^*} = 0$ and the pair (f,f^*) is related by the well known discrete *Koenigs duality* [4]. If \mathcal{M} is a ‘spherical’ Koenigs net, then the transformed mesh \mathcal{M}^* , the *dual*, exists and is a discrete minimal surface. Non-corresponding diagonals are parallel, i.e., $f_3^* - f_1^* \parallel f_4 - f_2$ and $f_4^* - f_2^* \parallel f_3 - f_1$.

$\alpha\beta = 0$: Even though we have excluded case where α or β takes the value 0, we can still interpret how Equation (10) transforms the quadrilateral. In this case each quadrilateral f of \mathcal{M} is transformed into a quadrilateral f^* of \mathcal{M}^* with parallel diagonals, since inserting $\alpha = 0$ (or analogously $\beta = 0$) into (11) yields for the directions of the two diagonals (recall $\sigma^2 = 1$)

$$d_1 = \beta \left(\frac{e_1}{\sqrt{p}} - \sigma \frac{e_2}{a_1 a_3} \right) \quad \text{and} \quad d_2 = \beta \left(\frac{e_2}{\sqrt{p}} - \sigma \frac{e_1}{a_2 a_4} \right) = -\frac{\sigma \beta \sqrt{p}}{a_2 a_4} \left(\frac{e_1}{\sqrt{p}} - \sigma \frac{e_2}{a_1 a_3} \right),$$

and thus parallelity. Planar quadrilateral nets with that property are called *T-nets* or *Moutard-nets* and play an important role in discrete differential geometry. It turns out that these special T-nets have vanishing oriented area (i.e., $\text{area}(f^*) = 0$) which can easily be verified by inserting $\alpha\beta = 0$ into Equation (21).

3.6 The Gauss map as discrete Cauchy problem

In this section we investigate the problem of finding a net \mathcal{M} which is a Gauss map of a net \mathcal{M}^* with constant ratio of principal curvatures but without knowing \mathcal{M}^* . And in particular we are interested in how many degrees of freedom we have or how much data for the appropriate initial values problem we can prescribe. We will have to consider different settings: general and circular nets as well as positive and negative ratios $\alpha : \beta$.

Interestingly, it appears that it is more easy to show the existence of a solution to the Cauchy problem in the more restricted case of circular nets, than for the more general case of non-circular nets.

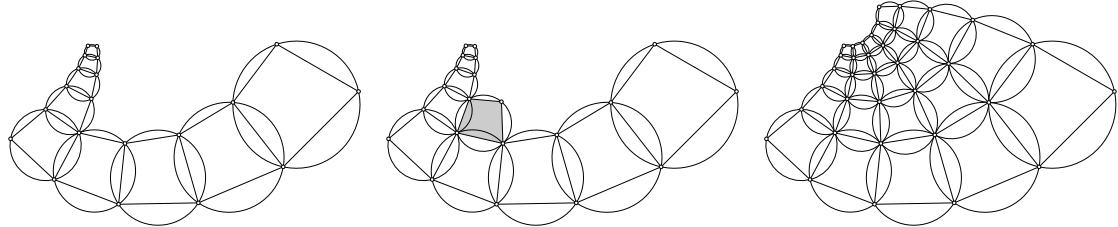


Fig. 7 Schematic image of a discrete Cauchy problem: Two given ‘orthogonally’ intersecting strips of circular quadrilaterals (left) can be extended to a mesh \mathcal{M} fulfilling the integrability condition (15) in the case of $\alpha\beta < 0$, i.e., \mathcal{M} is the Gauss map of a net \mathcal{M}^* with negative constant ratio of principal curvatures.

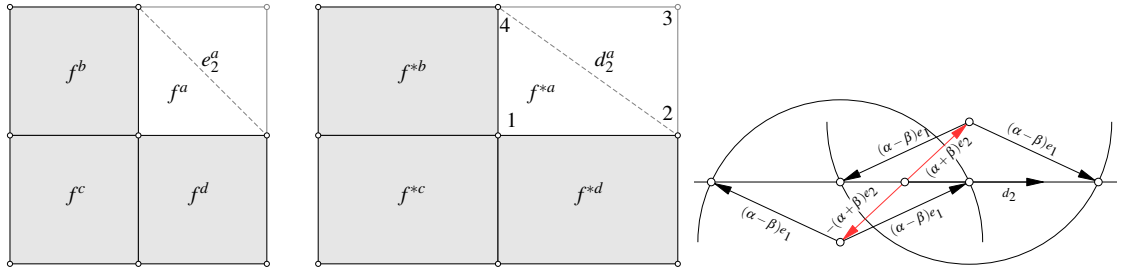


Fig. 8 *Left:* Schematic image of adding a remaining face f^a around a vertex (left) s.t. the resulting net contains this 2×2 faces as part of a Gauss map \mathcal{M} of a net \mathcal{M}^* (right) with a negative constant ratio of principal curvatures. *Right:* This image illustrates the simple geometric fact that for given d_2, e_2, α, β with $\|e_2\| = 1$ there always exists e_1 with $\|e_1\| = 1$ such that $(\alpha - \beta)e_1 \pm (\alpha + \beta)e_2 = \rho d_2$ if $|\alpha - \beta| \geq |\alpha + \beta|$.

Theorem 30. Suppose we are given two ‘orthogonally intersecting’ strips of circular quadrilaterals (see Fig. 7 left). Then these two strips can be extended to a rectangular patch with \mathbb{Z}^2 combinatorics such that \mathcal{M} is the Gauss map of a net \mathcal{M}^* with a negative constant ratio of principal curvatures.

Proof. Consider the three faces f^b, f^c, f^d of \mathcal{M} around the vertex where the two given strips meet (see Fig. 7). These faces can always be transformed (via Equation (10) plus appropriate scaling) to three faces f^{*b}, f^{*c}, f^{*d} of a mesh \mathcal{M}^* which we are looking for. What remains to show is that we can construct the missing face f^a around the same vertex to fill in the gap in such a way that a corresponding face f^{*a} would exist on a potentially transformed mesh \mathcal{M}^* (i.e., without leaving any gaps or overlaps).

From the three faces f^b, f^c, f^d we can read off the direction e_2^a that f^a would have (see Fig. 8 left) and similarly from the three faces f^{*b}, f^{*c}, f^{*d} we can read off the direction d_2^a of the diagonal that f^{*a} would have. And since we are in the ‘circular’ case (Proposition (24)) the direction d_2^a has then to be composable by the diagonals of f_a via Equation (19):

$$\rho d_2^a = (\alpha - \beta)e_1^a + \epsilon \sigma(\alpha + \beta)e_2^a,$$

for some $\rho \in \mathbb{R}$. Recall that e_1^a, e_2^a are unit vectors. So the entire existence question reduces to the question if such a vector e_1^a exists such that the above equation is fulfilled. For that it is best to look at Fig. 8 (right): the normalized vector e_1^a exists if the circle through the tip of e_2^a with radius $|\alpha - \beta|$ intersects the line with direction d_2^a .

Now the *negativity* of the ratio of the principal curvatures is important. It implies $\alpha < 0 < \beta$ or $\alpha > 0 > \beta$. In both cases we have $|\alpha + \beta| \leq ||\alpha| + |\beta|| = |\alpha - \beta|$. Consequently, the above mentioned circle intersects the line with direction d_2^a which gives us two possibilities to choose e_1^a . \square

In the case of *non-circular* nets we have even more degrees of freedom in the Cauchy problem considered in Theorem 30.

4 Discretization with asymptotic nets (A-nets)

In this section, we study a discretization of asymptotic nets on surfaces with a constant ratio of principal curvatures. As asymptotic lines exist only through hyperbolic points, we assume all surfaces here to have negative Gaussian curvature ($K < 0$). Therewith, there are two asymptotic lines passing through each point, forming an *asymptotic net* or *A-net*. In the case of a constant ratio of principal curvatures, these asymptotic lines intersect each other at a constant angle $\varphi = 2 \arctan \sqrt{-\kappa_1/\kappa_2} \stackrel{(1)}{=} \arctan \sqrt{-\beta/\alpha} = \text{const}$. Our goal is therefore to discretize a smooth A-net with constant intersection angles between their parameter lines.

We first need to fix some notation. We consider nets in \mathbb{R}^3 with \mathbb{Z}^2 -combinatorics: $f : \mathbb{Z}^2 \rightarrow \mathbb{R}^3$. Since we focus on local properties of nets we will omit, where possible, the parameter values $u \in \mathbb{Z}^2$ and use the common abbreviations: $f = f(u_1, u_2)$, $f_1 = f(u_1 + 1, u_2)$, $f_2 = f(u_1, u_2 + 1)$, $f_{12} = f(u_1 + 1, u_2 + 1)$, $f_{\bar{1}} = f(u_1 - 1, u_2)$, etc. And, the following discretization of A-nets appears several times in discrete differential geometry (cf. [3, 19]).

Definition 31. A *discrete asymptotic net* or *discrete A-net* is a map $f : \mathbb{Z}^2 \rightarrow \mathbb{R}^3$, wherein each vertex star is planar, i.e., the five points $f, f_1, f_2, f_{\bar{1}}, f_{\bar{2}}$ lie in a plane (Fig. 9, left). Along with that, the edges will be denoted $\Delta_j f := f_j - f$ for each of $j \in \{1, \bar{1}, 2, \bar{2}\}$, the one-ring neighbors of f .

This definition is formulated in such a way that the discrete parameter lines $\{f(u_1 + k, u_2)\}_{k \in \mathbb{Z}}$, and $\{f(u_1, u_2 + k)\}_{k \in \mathbb{Z}}$, are discrete asymptotic lines.

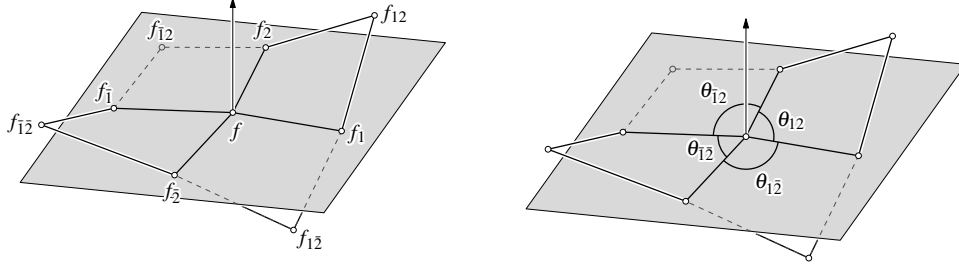


Fig. 9 *Left:* A-net with labelling of a vertex's one-ring neighbors. *Right:* Labelling of the angles around a regular vertex.

4.1 Formulation

Here we will formulate the conditions on a net $f : \mathbb{Z}^2 \rightarrow \mathbb{R}^3$ so that it is a discrete A-net emulating a surface which has a discretized constant ratio of principal curvatures.

For the net to be an A-net, it must, by definition, have planar vertex stars. To facilitate this, a vertex normal n_f is used, so that the planarity at f can be written as

$$n_f \cdot \Delta_j f = 0 \quad (22)$$

for each of $j \in \{1, \bar{1}, 2, \bar{2}\}$.

Consider now the interior vertices f of the net. Since a constant ratio of principal curvatures is equivalent to the asymptotic lines having a constant angle $\varphi = 2 \arctan \sqrt{-\kappa_1/\kappa_2}$ between them, we discretize this condition in the following way. Let $0 \leq \theta_{jk} < \pi$ be the angle between the edges $\Delta_j f$ and $\Delta_k f$, as shown in Fig. 9, right. Then, since the vertex star is necessarily planar, and thus, the angles sum to 2π , we require that the following conditions on the averages of the angles hold

$$\begin{aligned} \theta_{12} + \theta_{\bar{1}\bar{2}} &= 2\varphi \quad \text{and} \quad \theta_{2\bar{1}} + \theta_{\bar{2}1} = 2(\pi - \varphi) \\ \text{or} \\ \theta_{12} + \theta_{\bar{1}\bar{2}} &= 2(\pi - \varphi) \quad \text{and} \quad \theta_{2\bar{1}} + \theta_{\bar{2}1} = 2\varphi. \end{aligned}$$

In order to resolve this ambiguity in that or statement, we can use the periodicity of cosine to obtain

$$\cos(\theta_{12} + \theta_{\bar{1}\bar{2}}) = \cos 2\varphi = \cos 2(\pi - \varphi) = \cos(\theta_{2\bar{1}} + \theta_{\bar{2}1}), \quad (23)$$

which is to say that the cosines the sums of opposite angles are equal, having a value of $\cos 2\varphi$.

4.2 Formulation as zeros of at-most-quadratic functions

The method of optimization is taken from Tang et al. [22], which requires that the constraints are at-most-quadratic. To ensure that they are at-most-quadratic and so that there are no degenerate solutions, auxiliary variables are used. Here, we will outline such constraints for A-nets, which also meet the angle condition, Equation (23).

For the planarity of the vertex stars constraint, Equation (22), it must be that n_f and $\Delta_j f$ are non-zero; to ensure this, we assert that n_f is a unit vector, and that the auxiliary variable F_j is the unit edge. This turns Equation (22) into the following group of equations:

$$\begin{aligned} n_f \cdot n_f &= 1 \\ F_j \cdot F_j &= 1 \\ \Delta_j f \cdot \Delta_j f &= l_{\Delta_j f}^2 && \text{auxiliary variable } l_{\Delta_j f} \text{ for the edge length} \\ l_{\Delta_j f} F_j &= \Delta_j f && \text{to connect the unit edge with the edge} \\ l_{\Delta_j f}^2 &= d_{\Delta_j f}^2 && \text{auxiliary variable } d_{\Delta_j f} \text{ to ensure } l_{\Delta_j f} \geq 0 \\ n_f \cdot F_j &= 0. \end{aligned}$$

To translate Equation (23) for interior vertices, auxiliary variables are needed to handle the higher-order function cosine. In order to do this, the equations will first be reduced using the angle-sum identity for cosine,

$$\cos(\alpha + \beta) = \cos \alpha \cos \beta - \sin \alpha \sin \beta.$$

As such, Equation (23) turns into the following: using the auxiliary variable c_{jk} and s_{jk} to stand in for the cosine and sine, respectively,

$$\left. \begin{cases} c_{jk} = F_j \cdot F_k = \cos \theta_{jk} \\ s_{jk}^2 = 1 - c_{jk}^2 \end{cases} \right\} \quad \text{for } jk \in \{12, \bar{1}\bar{2}, 2\bar{1}, \bar{2}1\}$$

$$\begin{aligned} c_{12}c_{\bar{1}\bar{2}} - s_{12}s_{\bar{1}\bar{2}} &= \cos 2\varphi \\ c_{2\bar{1}}c_{\bar{2}1} - s_{2\bar{1}}s_{\bar{2}1} &= \cos 2\varphi. \end{aligned}$$

4.3 Method of optimization, propagating these A-nets from a strip

In this section, we will give an overview of how we obtained examples of these A-nets of a constant ratio of principle curvatures. For the optimization, the methodology, outlined by Tang et al. [22], was used with the at-most-quadratic formulation in the previous section. And to facilitate the formation of these surfaces, we have devised a means to propagate these surfaces from a strip of quads, as detailed below.

Given a smooth curve $\gamma: [t_0, t_N] \rightarrow \mathbb{R}^3$, with a partition $t_0 < t_1 < \dots < t_N$, and an initial orthonormal frame at $\gamma(t_0)$, we devised a method for generating quads along γ , with the aim that it is reasonable enough to be optimized for the vertex-star planarity, and angle, condition. To do this, first, frames at all points t_j of the partition are constructed in a rotation-minimizing way, following the method outlined in [8, §II.B]. Here, the initial frame comprises the unit tangent vector $\hat{\gamma}'(t_0)$, a chosen vector $\hat{n}(t_0)$, and the mutually-orthogonal vector $\hat{n}(t_0) \times \hat{\gamma}'(t_0)$, as depicted in Fig. 10, left. Then, the frame at $\gamma(t_{j+1})$ is gotten from the one at $\gamma(t_j)$ by rotating it about the vector $\hat{\gamma}'(t_j) \times \hat{\gamma}'(t_{j+1})$ by the angle $\arccos \hat{\gamma}'(t_j) \cdot \hat{\gamma}'(t_{j+1})$; let this rotation be denoted by T_j , so that $T_j \hat{\gamma}'(t_j) = \hat{\gamma}'(t_{j+1})$, and so on. Thusly, a frame is obtained at each point $\gamma(t_j)$, for $0 \leq j \leq N$.

With these frames, vertices are then added, allowing for the addition of faces between each of the pairs of points $\gamma(t_j)$ and $\gamma(t_{j+1})$. To facilitate this, at each $\gamma(t_j)$, there is a plane P_{t_j} normal to $\hat{n}(t_j)$, which is

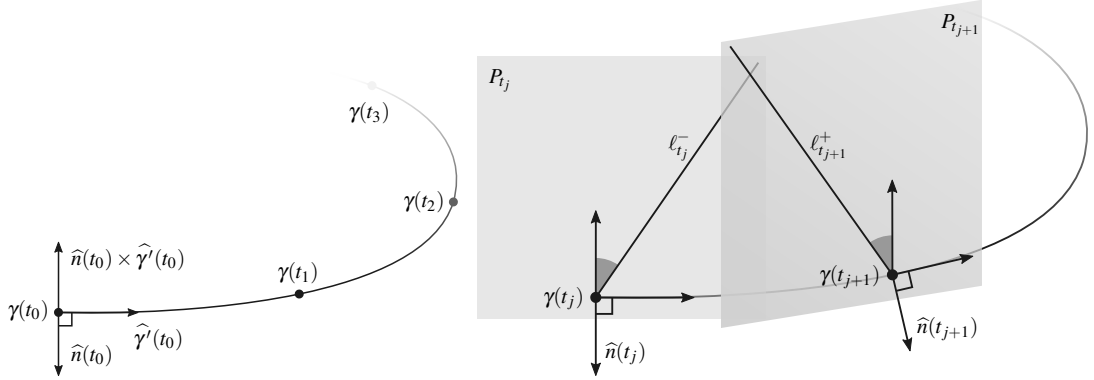


Fig. 10 *Left:* A given smooth curve with a partition $t_0 < t_1 < \dots < t_N$, and an initial orthonormal frame at $\gamma(t_0)$. *Right:* Planes at both $\gamma(t_j)$ and $\gamma(t_{j+1})$, which are perpendicular to $\hat{n}(t_j)$, and $\hat{n}(t_{j+1})$, respectively, and which contain the lines $\ell_{t_j}^-$, and $\ell_{t_{j+1}}^+$, respectively.

spanned by $\{\hat{\gamma}'(t_j), \hat{n}(t_j) \times \hat{\gamma}'(t_j)\}$. Let $0 < \tau < \frac{\pi}{2}$ to be the target angle. Using this angle, let $\ell_{t_j}^-$ be the line in that plane at $\gamma(t_j)$, which forms an angle of $-(\frac{\pi}{2} - \tau)$ with $\hat{n}(t_j) \times \hat{\gamma}'(t_j)$, and let $\ell_{t_{j+1}}^+$ be the line in the plane at $\gamma(t_{j+1})$, which forms an angle of $+(\frac{\pi}{2} - \tau)$ with $\hat{n}(t_{j+1}) \times \hat{\gamma}'(t_{j+1})$, see Fig. 10, right. The line $\ell_{t_{j+1}}^+$ at $\gamma(t_{j+1})$ is then rotated back by the rotation T_j , to obtain the line

$$\check{\ell}_{t_{j+1}}^+ := T_j^{-1}(\ell_{t_{j+1}} - \gamma(t_{j+1})) + \gamma(t_{j+1})$$

at $\gamma(t_{j+1})$, which lies in the in the plane

$$\check{P}_{t_{j+1}} := T_j^{-1}(P_{t_{j+1}} - \gamma(t_{j+1})) + \gamma(t_{j+1}),$$

parallel to P_{t_j} by the construction of T_j . Therewith, a new “upper” vertex v_j^u is added as the point which is closest to both $\ell_{t_j}^-$ and $\check{\ell}_{t_{j+1}}^+$. This process is then repeated, using the line $\ell_{t_j}^+$ and $\check{\ell}_{t_{j+1}}^-$, to obtain a new “lower” vertex v_j^l as the point which is closest to them both. The new face is then given by the vertices $\{\gamma(t_j), v_j^l, \gamma(t_{j+1}), v_j^u\}$; see Fig. 11, left, for an illustration.

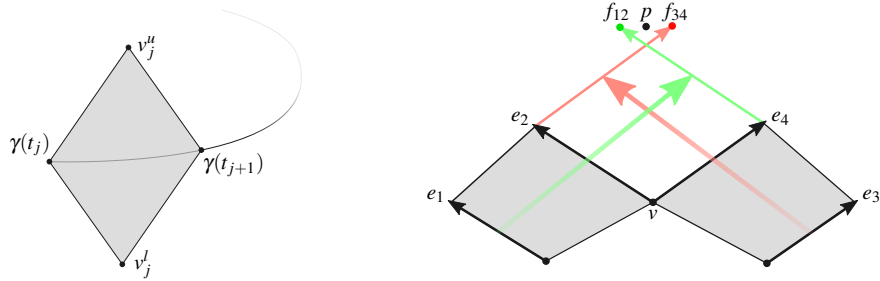


Fig. 11 *Left:* Face added along the curve. *Right:* Propagation of faces.

In order to obtain a more substantial surface, a method of propagating these strip by adding faces was developed, with the aim of the result being optimized to more-closely attain the constraints for these A-nets. To add a face “opposite” a vertex, say, v , consider the edge vectors e_1, e_2, e_3, e_4 , as shown in Fig. 11, right. Two suggestions for the new vertex p to complete the new face, are constructed from the vectors f_{12} and f_{34} , which are such that the second differences of $\{e_1, e_2, f_{12}\}$, and $\{e_3, e_4, f_{34}\}$, are zero — namely,

$f_{12} = 2e_2 - e_1$ and $f_{34} = 2e_4 - e_3$. Lastly, p is taken to be the average of $f_{12} + e_4 + v$ and $f_{34} + e_2 + v$, to complete the face $\{v, e_4 + v, p, e_2 + v\}$.

4.4 Support structure generation

In this section, we will discuss how the support structures for these surfaces are generated, as described in [21]. Along each polyline, there is a discrete developable surface, with straight development. To form these surfaces, rulings will be calculated for each of the two polylines passing through each vertex that is sufficiently far from the edge of the mesh.

Using the notation in Fig. 12, the (unit) tangent vector $t(v_j)$ at the vertex v_j is computed as

$$t(v_j) := \frac{(v_{j+1} - v_j) \times n(v_j)}{|(v_{j+1} - v_j) \times n(v_j)|},$$

where $n(v_j)$ is the vertex normal at v_j . Therewith, the ruling vector $r(v_j)$ at the vertex v_j , is computed by

$$r(v_j) := s \cdot (t(v_{j-1}) \times (t(v_j) + t(v_{j+1}))) + v_j,$$

where s is a sign determined as to keep $r(v_j)$ on a consistent side of the surface. As one can see, these computations requires that the vertex v_j is sufficient far from the edge of the mesh. To obtain the support structure, these ruling vectors are used along with the vertices of the original mesh, to extrude the discrete developable surfaces of the support structure.

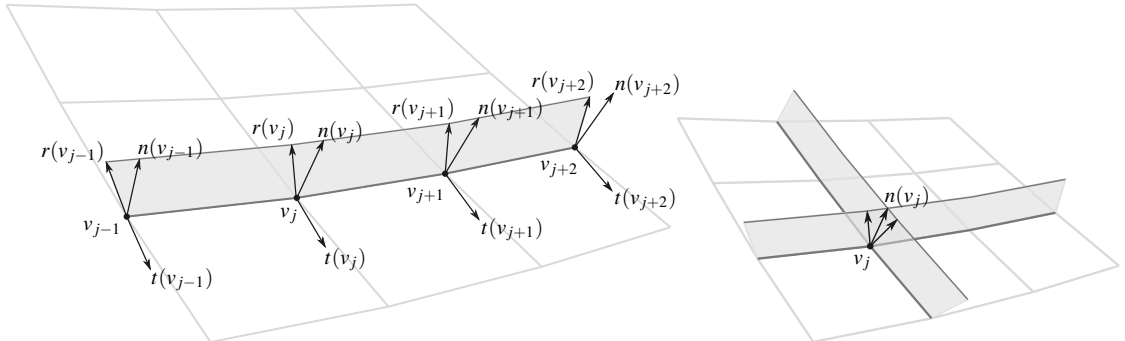


Fig. 12 *Left:* One of the developables through v_j , including the vertex normals, tangent vectors, and ruling vectors. *Right:* Both developables through v_j , including the vertex normal and both ruling vectors.

4.5 Examples

The most readily-available examples are surfaces of revolution, which can be obtained from an integral [11, §3.27]. To obtain more examples, the results on generalized Chebyshev nets with a constant Chebyshev angle from the papers by Riveros and Corro, [17] and [18], were used to integrate boundary data, which was then propagated, and optimized, in succession.

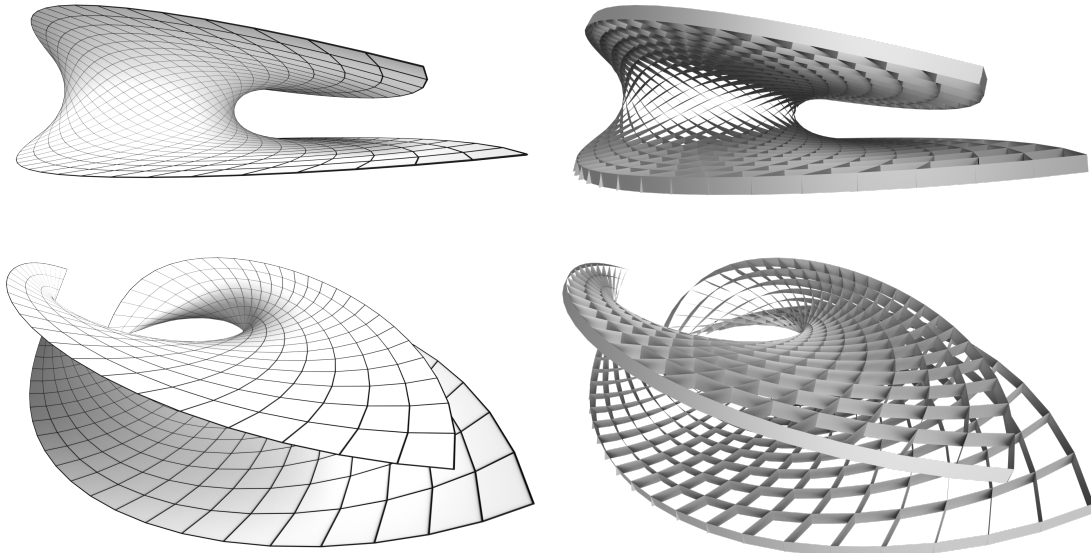


Fig. 13 An A-net with an angle of $\pi/3$, and its accompanying support structure.

Acknowledgements

The authors would like to thank Udo Hertrich-Jeromin and Mason Pember for useful discussions, and greatly acknowledge the support of the Austrian Science Fund (FWF) through projects P 29981 and I 2978, and by the EU Framework Program Horizon 2020 under grant 675789 (ARCADES).

References

1. W. Blaschke and G. Bol. *Geometrie der Gewebe. Topologische Fragen der Differentialgeometrie*. Springer, 1938.
2. A. I. Bobenko, H. Pottmann, and J. Wallner. A curvature theory for discrete surfaces based on mesh parallelity. *Math. Ann.*, 348(1):1–24, 2010.
3. A. I. Bobenko and Yu. B. Suris. *Discrete differential geometry. Integrable structure*, volume 98 of *Graduate Studies in Mathematics*. American Mathematical Society, 2008.
4. A. I. Bobenko and Y. B. Suris. Discrete Koenigs nets and discrete isothermic surfaces. *Int. Math. Res. Not.*, (11):1976–2012, 2009.
5. E. B. Christoffel. Ueber einige allgemeine Eigenschaften der Minimumsflächen. *J. Reine Angew. Math.*, 67:218–228, 1867.
6. M. Eigensatz, M. Kilian, A. Schiftner, N. Mitra, H. Pottmann, and M. Pauly. Paneling architectural freeform surfaces. *ACM Trans. Graphics*, 29(4):#45, 1–10, 2010. Proc. SIGGRAPH.
7. L. P. Eisenhart. *An Introduction to Differential Geometry*. Princeton Mathematical Series, v. 3. Princeton University Press, 1940.
8. A. J. Hanson and H. Ma. Quaternion frame approach to streamline visualization. *IEEE Transactions on Visualization and Computer Graphics*, 1(2):164–174, June 1995.
9. H. Hopf. Über Flächen mit einer Relation zwischen den Hauptkrümmungen. *Math. Nachr.*, 4:232–249, 1951.
10. O. N. Karpenkov. On the flexibility of Kokotsakis meshes. *Geometriae Dedicata*, 147(1):15–28, 2010.
11. W. Kühnel. *Differentialgeometrie*. Aufbaukurs Mathematik. Springer Spektrum, Wiesbaden, updated edition, 2013. Kurven—Flächen—Mannigfaltigkeiten.
12. E. P. Lane. Bundles and pencils of nets on a surface. *Trans. Amer. Math. Soc.*, 28(1):149–167, 1926.
13. I. M. Mladenov and J. Oprea. The Mylar balloon revisited. *Amer. Math. Monthly*, 110(9):761–784, 2003.
14. I. M. Mladenov and J. Oprea. The Mylar balloon: new viewpoints and generalizations. In *Geometry, Integrability and Quantization*, pages 246–263. Softex, Sofia, 2007.
15. C. Müller and J. Wallner. Oriented mixed area and discrete minimal surfaces. *Discrete Comput. Geom.*, 43(2):303–320, 2010.
16. H. Pottmann, M. Eigensatz, A. Vaxman, and J. Wallner. Architectural geometry. *Computers and Graphics*, 47:145–164, 2015.

17. C. M. C. Riveros and A. M. V. Corro. Surfaces with constant Chebyshev angle. *Tokyo J. Math.*, 35(2):359–366, 2012.
18. C. M. C. Riveros and A. M. V. Corro. Surfaces with constant Chebyshev angle II. *Tokyo J. Math.*, 36(2):379–386, 2013.
19. R. Sauer. *Differenzengeometrie*. Springer-Verlag, Berlin-New York, 1970.
20. C. Tang, M. Kilian, P. Bo, J. Wallner, and H. Pottmann. Analysis and design of curved support structures. In *Advances in Architectural Geometry 2016*, pages 8–23. VDF Hochschulverlag, ETH Zürich, 2016.
21. C. Tang, M. Kilian, P. Bo, J. Wallner, and H. Pottmann. Analysis and design of curved support structures. In S. Adriaenssens, F. Gramazio, M. Kohler, A. Menges, and M. Pauly, editors, *Advances in Architectural Geometry 2016*, pages 8–23. VDF Hochschulverlag, ETH Zürich, 2016.
22. C. Tang, X. Sun, A. Gomes, J. Wallner, and H. Pottmann. Form-finding with polyhedral meshes made simple. *ACM Trans. Graphics*, 33(4):70:1–70:9, 2014. Proc. SIGGRAPH.